Evaluation of Histomorphometric Changes in the Small Intestinal Epithelium and Paneth cells of Male Sprague Dawley Rats Exposed to Alcohol and/or Combination Anti-Retroviral drug (Atripla)Therapy (cART)

UNIVERSITY OF THE WITWATERSRAND, JOHANNESBURG

Student name: Zekhethelo Leticia Maseko

Student number:1837647

Degree: MSc. Medicine

Supervisor: Dr P Mazengenya

Co-supervisors: Prof T Luvhengo & Prof EF Mbajiorgu

School of Anatomical Sciences, Faculty of Health Sciences, University of the Witwatersrand, 7 York Road, Park Town, Johannesburg 2193

DECLARATION

I, Zekhethelo Leticia Maseko declare that this thesis is my own, unaided work. It is being submitted for the Degree of Master of Science in Medicine at the University of the Witwatersrand, Johannesburg. It has not been submitted before for

any degree or examination at any other University.

_____

31th day of March 2022 in Johannesburg, Gauteng

DEDICATION

I dedicate this research to my late sister, Noxolo Carol Mahlangu who will always be remembered for her passion for education and success in life.

ABSTRACT

Significant number of individuals who have HIV/AIDS are also chronic alcohol consumers (Pandrea et al., 2010). Alcohol intake has been found to disrupts ARV drug bioconversion and innate immunity of the gut (Bishehsari et al., 2017), but the exact effects of the combined use of alcohol and/or cARV on small intestinal epithelium and Paneth cells remains unclear. Paneth cells are the main regulator of innate immunity of the gut (Salzman et al., 2010). This study evaluated the histomorphologic appearances of Paneth cells and crypt-villous morphology in small intestine of rats exposed to alcohol and/or combination anti-retroviral drug therapy (cART).

The study utilized an experimental study design of 32 adult male Sprague-Dawley rats which were divided into 4 groups and treated with normal saline, alcohol, cART or a combination of alcohol and cART. The animals were sacrificed after 90 days. Segments of small intestine were collected and studied to evaluate the morphometric changes of crypts and villi dimensions in the jejunum and ileum, determine the location of the Paneth cells along the axis of the intestinal crypts of the jejunum and ileum. Furthermore, to examine the histomorphological appearance of Paneth cells including their morphology and amounts of secretory granules, in the jejunum and ileum and examine the histomorphological appearance of stem cells in the crypts of the jejunum and ileum using H&E,special stains and immunohistochemistry. Histomorphometric measurements were done using ImageJ software. Analysis of data was done using STATA SE 15 statistical software.

Morphometry and morphological analysis showed significant ($p < 0.05$) reduction in villous height, villous width, crypt's depth, intestinal stem cells, increased villous stripping, increased crypt's width, increased muscular wall thickness, increased number of Paneth cells and staining intensity of Paneth cell granules in alcohol + cART treated group. The increase in number of villi was in all experimental groups and highest following treatment with cART alone or in combination with alcohol. The shortest villi, shallowest crypts and the least number of crypts were seen in ileum of animals that had cART alone. The alcohol alone group had the least number of villi but showed increased collagen content. Paneth cells were noted in the proliferation zone of intestines of animals that had combined treatment (alcohol +cART).

Concomitant use of alcohol and cART led to thickening of small intestinal wall, shortening and/or stripping the villi, reduction of crypt depth, appearance of Paneth cells in proliferation zone and a

decrease in intestinal stem cells. The structural changes in the small intestine and Paneth cells may adversely affect the regulation of gut innate immunity. These findings are clinically invaluable in the management of HIV patients considering the critical significance of innate immunity amongst HIV patients.

ACKNOWLEDGEMENTS

Throughout the study, I was guided, advised, assisted, encouraged, motivated, and supported by various people in numerous ways. My appreciation and acknowledgements go to:

- *My Supervisor, Dr. P Mazengenya for his patience, diligent guidance, and encouragement throughout the study.*
- *My co-supervisor, Prof E Mbajiorgu for the incredible support, guidance, and encouragement he gave during the study.*
- *My co-supervisor, Prof T Luvhengo for his encouragement and willingness to assist throughout the research process.*

Table of Contents

LIST OF ACRONYMS / ABBREVIATIONS

ABPAS	Alcian blue–periodic Acid-Schiff
ADH	Alcohol dehydrogenase
AIDS	Acquired immunodeficiency syndrome.
ALD	Alcoholic liver disease
AMP	Anti-microbial proteins
ARV	Antiretroviral therapy
cART	Combination Antiretroviral therapy
CC	Collagenous colitis
CD	Celiac disease
CSC	Cancer stem cells
DAB	3,3′-Diaminobenzidine
GIT	Gastrointestinal tract
H&E	Haematoxylin and eosin stain
HD-5	Human defensin-5
HD-6	Human defensin-6
HIV	Human immunodeficiency virus
IHC	Immunohistochemistry
IL	Interleukin
INSTI	Integrase strand transfer inhibitors
MT	Masson Trichrome
NNRTI	Nonnucleoside reverse transcriptase inhibitors
NRTI	Nucleoside reverse transcriptase inhibitors
PC	Paneth cells
PI	Protease inhibitors
SIV	Simian immunodeficiency virus
TNF	Tumour necrosis factor

LIST OF FIGURES

LIST OF TABLES

CHAPTER 1: INTRODUCTION

South Africa (RSA) has proportionally the largest human immunodeficiency virus (HIV) positive population in the world with an estimated prevalence rate of 13% and 7,8 million people living with HIV in 2020 alone (Cihlar and Fordyce, 2016, Mah et al., 2014). In addition, RSA has the largest combination anti-retroviral therapy (cART) program in the world (Boulle et al., 2008). cART program has improved the quality of life of HIV infected individuals. The cART has also led to a reduction in occurrence of gastrointestinal (GIT) symptoms and complications which were commonly associated with chronic HIV disease (Cihlar and Fordyce, 2016). The GIT symptoms and complications in HIV positive patients were due to what is now referred to as "HIV enteropathies" (Kotler et al., 1984). The histological changes seen in HIV enteropathy include villous atrophy, crypt hyperplasia and epithelial hypo-proliferation (Kotler, 2005).

cART program has improved the quality of life of HIV infected individuals but there is still limited information on how different antiretroviral drugs affect the mucosa of GIT when combined with alcohol. The current evidence suggests that cART ameliorates damage to the intestinal epithelium which is caused by HIV infection, particularly if treatment is initiated during early stages of the infection (Brenchley and Douek, 2008).

Significant advances have been made in the development of cART drugs since the introduction of zidovudine (AZT) in the year 1987 (Cihlar and Ray, 2010) and currently there are more than 30 combination anti-retroviral drugs. Antiretroviral (ARV) drugs are categorized into six classes (Kallings, 2008). Each ARV drug targets a specific phase in replication of HIV (Voshavar, 2019). To ensure an effective therapeutic response with lower risk of development of resistance, drugs from two or sometimes three classes are combined, an example of such a combination drug is Atripla (Cihlar and Ray, 2010). Atripla is a once a day three-drug fixed-dose combination tablet used to treat HIV infection (Cohen et al., 2011). It consists of 600 mg of efavirenz (EFV), 200 mg of emtricitabine (FTC) and 300 mg of tenofovir disoproxil fumarate (Boulle et al., 2008). Efavirenz belongs to non-nucleoside reverse transcriptase inhibitors (NNRTI) (Bagasra et al., 1993, Voshavar, 2019) whereas emtricitabine and tenofovir belong to nucleoside reverse transcriptase inhibitors (NRTI) group (Cihlar and Ray, 2010).

Recent reports have suggested that the use of alcohol or recreational drugs is related to sexual behavior which has been shown as a high-risk factor for HIV infection. Reports have also shown that the abuse of alcohol hinders patient's adherence to cARV drug schedule and therefore leads to disease progression to AIDS(Bagasra et al., 1993, Bishehsari et al., 2017, Pandrea et al., 2010, Samet et al., 2007, Imhof et al., 2001). Furthermore, there is an association between alcohol abuse by individuals who are HIV positive with lower educational status and being males.

The combined use of alcohol and cARV drugs is not advisable since ARV drugs undergo significant metabolism in the liver, therefore, there is increased likelihood for alcohol to disrupt bioconversion of the drugs because of the combined effect on the enzymes found in the liver and intestines (Cihlar and Fordyce, 2016). The role of the liver is to oxidize small foreign organic molecules, such as toxins or drugs so that they can be removed from the body (McCance-Katz, 2016). The two most commonly used cART regiments inhibit Cytochrome P450 3A4 enzyme, causing the liver to failto effectively metabolize and remove alcohol from the body (Cihlar and Ray, 2010, Cihlar and Fordyce, 2016). One such inhibitor is Ritonavir, it inhibits Cytochrome P450 3A4 in the liver and intestines by increasing the effects of alcohol when taken concomitantly (McCance-Katz, 2016). Ritonavir is metabolized principally by Cytochrome P450 3A4 whereas Efavirenz is principally metabolized by CYP 2B6 and CYP 3A4. Drug to drug interactions might place patients at risk of toxicities or possibly to ineffective antiretroviral plasma concentrations and also to non-adherence to prescribed regimens (McCance-Katz, 2016). The same enzymes that are involved in the biotransformation of the ARV drugs into toxic intermediates are involved in the breakdown of alcohol (Cohen et al., 2011, Villanueva-Millan et al., 2017, Samet et al., 2007, Batman et al., 2014, McCance-Katz, 2016).

The combined use of cART and alcohol affects the working of the gut immune system through Paneth cells by inducing intestinal inflammation through a cascade of mechanisms that subsequently lead to general inflammation, organ dysfunction and possibly death (Bishehsari et al., 2017, Iyer and Vaishnava, 2016). Alcohol affects intestinal mucosal immunity by suppressing antibacterial activity of antimicrobial peptides and proteins which are secreted by Paneth cells (Bishehsari et al.,2017). When suppressed, Paneth cells secrete fewer antimicrobial compounds

which leads to the overgrowth of luminal bacteria and other pathogens, and subsequently translocation through the intestinal epithelium (Pandrea et al., 2010, Bishehsari et al., 2017).

Translocation of bacteria triggers an inflammatory response by the gut immune system which leads to a release of proinflammatory cytokines (Bishehsari et al., 2017). The endotoxins and cytokines can alter hepatic function by directly interacting with hepatocytes or the immune active cells in the liver (Bishehsari et al., 2017 (Samet et al., 2007). The immune activation leads to an increase in viral replication and poor ARV response, a vicious cycle that continues until death. However, there is a paucity of information and or studies on the effects of concomitant use of alcohol and cART particularly ATRIPLA on the small intestines in experimental animals. The purpose of the current study is therefore to investigate the histomorphological changes in the small intestines and Paneth cells of male Sprague-Dawley rats following exposure to alcohol with or without cART treatment.

.

CHAPTER 2: LITERTURE REVIEW

2.1 Introduction

In this chapter the literature on HIV enteropathy, small intestines, Paneth cells and the mechanisms of action of Paneth cells in viral infections are examined in detail. The literature on the combination of cART and alcohol on Paneth cells regulation of the innate immune system of the gut with focus on HIV enteropathy and its implications are discussed.

2.2 HIV enteropathy

HIV enteropathy was first described in 1984, as a change in intestinal structure and function in HIV-infected individuals, HIV enteropathy is a syndrome without an identified malignancy or pathogen other than HIV (Kotler et al., 1984). Manifestations of HIV enteropathy includes chronic diarrhea, increased intestinal inflammation, increased intestinal permeability and malabsorption of bile acid and vitamin B12 (Batman et al., 2007, Kotler et al., 1984). HIV enteropathy results from direct and indirect effects of the virus (Batman et al., 2007). The gp120, is a glycoprotein on HIV envelope; that negatively affects tubulin depolymerization and induces local production of pro-inflammatory cytokines such as interleukin 6, interleukin 10 and tumor necrosis factor (Cello and Day, 2009).

The effects of HIV on the gut mucosa may lead to an altered epithelial ionic balance and apoptosis of enterocytes (Zeitz et al., 1998, Batman et al., 2007) which may cause structural and/or immunological abnormalities (Batman et al., 2007). The histological changes which have been reported in small intestine following HIV infection include villous atrophy, crypt hyperplasia, epithelial hypoproliferation and CD+ T cells depletion within the lamina propria (Bjarnason et al., 1996, Zeitz et al., 1998, Johanson, 1996).

2.3 Microanatomy of the small intestines

The small intestine is made up of four layers that include mucosa, submucosa, muscularis and outermost serosa (Egorov et al., 2002). The mucosa of small intestine is lined by simple columnar

epithelium (Clevers and Bevins, 2013). The mucosa is thrown into permanent folds called plicae circulares (Egorov et al., 2002). From the plicae circulares project microscopic villi (Clevers and Bevins, 2013). The individual epithelial cells possess microvilli on their apical surfaces, which together with plicae circulares and villi they increase the surface area for absorption (Johnson,1988).

The epithelium of small intestine lines its luminal surface which has crypts and villi containing four major cell types. The cells include absorptive enterocytes which make up greater than 80% of the total population, goblet cells, Paneth cells and enteroendocrine cells which are all derived from the intestinal stem cell (Yokoi et al., 2019). Mature enterocytes are tall and columnar in shape and are found on the villous surface, the enterocytes have apical microvilli and are responsible for the absorption of nutrients (McCauley et al., 2020). The goblet cells are second most populous cell type and are responsible for the secretion of mucin which mixes with water to form mucus (Clevers and Bevins, 2013).

Enteroendocrine cells are located within Crypts of Lieberkühn, that secrete hormones in response to various stimuli Gunawardene et al.,2011) There are four main classes of enteroendocrine cells, each with a different secretory product (Yokoi et al., 2019). These are I cells, S cells, K cells and enterochromaffin cells (Gunawardene et al., 2011). The intestinal stem cells are found at stem cell zone which is an area towards the base of intestinal crypts (Yokoi et al., 2019).

2.4 Paneth cell structure and function

Paneth cells(PCs) are pyramidal formed cells with prominent eosinophilic granules (Ehrmann et al., 1990). They have a broad base which rests on basement membrane and are narrow towards the apical end (Yokoi et al., 2019). Their nucleus is irregularly shaped and occupies a third of the basal cytoplasm (Ehrmann et al., 1990). Brush borders are identified on their apical surface and secretory granules of variable sizes are found in apical part of the cytoplasm (Al-Saffar, 2016). The remainder of the cytoplasm of PCs contains well established granular endoplasmic reticulum in paranuclear region of cells and Golgi apparatus located in the supranuclear region (Ehrmann et al., 1990).

Each intestinal crypt in humans contains 30-50 mature PCs that survive for about 18-23 days before degenerating (Garabedian et al., 1997). Unlike the rest of differentiated cells which migrate upwards in the crypts, PCs migrate towards the crypt base and have a lifespan of more than three weeks (Ganz, 2000). The position of PCs in crypts is directly proportional to their age, with more mature cells occupying the base of the crypts (Dipankar Ghosh, 2000). The size of a Paneth granules can also give an estimate of its age, with larger granules being found in older cells (Garabedian et al., 1997).

The intestinal epithelium plays a critical role in host defense and is among the key players in gut immunity (Al-Saffar, 2016, Ehrmann et al., 1990). PCs store and secrete immunoglobulins, lysozyme, and other anti-microbial peptides (Batman et al., 2007, Clevers and Bevins, 2013, Mei et al., 2020). The anti-microbial peptides which are stored in granules include α-defensins, lysozyme, secretory phospholipase A2 (sPLA2), angiogenin-4 (Ang4), RegIIIγ, and α1-antitrypsin. Enteric α-defensins are the most abundant of the secreted products (Lencer, 1998).

The anti-microbial peptides which are secreted by PCs have strong anti-microbial activities against a range of bacteria, fungi, parasites, and viruses (Holly et al., 2017). They determine the composition of gut microbiota. In addition, PC secretions are involved in the nourishment of stem cells and also keeping ISC zone sterile (Lencer, 1998). Furthermore, some of the secretions from PCs have trophic effects on other derivatives of ISCs (Lencer, 1998, Lueschow and McElroy, 2020).

The α-defensins are small, cationic, and amphipathic peptides with two β-sheets stabilized by three disulfide bonds, humans encode genes for two α-defensins namely human defensin 5 (HD5), and human defensin 6 (HD6), whereas mice encode over 25 different enteric α-defensin genes (Dipankar Ghosh, 2000, Lueschow and McElroy, 2020). Expression of subsets of α-defensin genes in mice are dependent on the strain (Yokoi et al., 2019). The extensive antimicrobial activity of HD5, including its potent antiviral activity, is well documented (Zapata et al., 2008, D'Agostino et al., 2009, Dipankar Ghosh, 2000). Human defensin 6 has a unique mode of action and functions by trapping bacteria and fungi.

The other antimicrobial constituents of PC granules are not known to be active against viruses, but lysozyme acts by cleaving peptidoglycan in cell walls of bacteria (Karlsson et al., 2008). Changes in the number of PCs in intestinal crypts, morphology, and their location along the crypt-villous

axis as well as in number and distribution cytoplasmic granule have been reported in some pathological conditions including coeliac disease and parasitic infestation (Lueschow and McElroy, 2020, Gassler, 2017, Garabedian et al., 1997, Kelly et al., 2004, Holly et al., 2017).

Antimicrobials secreted by PCs regulate the composition of intestinal microbiota and prevent colonization of intestinal crypt environment by pathogens (Dipankar Ghosh, 2000). Although anti-HIV activity of alpha, beta, and delta defensins have been reported, their role in controlling HIV infection is still unknown (Zapata et al., 2008). One intriguing area of research that warrants further investigation is the role of α-defensins in mitigating the effects of HIV-1 as the disease progresses (Yokoi et al., 2019). HIV-1 and simian immunodeficiency virus infection in human and animals, respectively induce inflammation by upregulating proinflammatory cytokine and chemokine expression by increasing intestinal permeability in GI tract (Llenado et al., 2009). The loss of α-defensin during HIV infection then leads to overgrowth of enteric pathogens resulting in gastrointestinal dysfunction (Yokoi et al., 2019).

2.5 Paneth cells in intestinal diseases

Around 10^{14} bacteria reside in a symbiotic relationship with host in the lumen of small intestine of a healthy adult human (Hirao et al., 2014). Each species of bacteria has its own tightly regulated niche (Salzman et al., 2010). Disruption of intestinal microbiota is called dysbiosis. Dysbiosis is associated with several diseases such as obesity, diabetes mellitus, cardiovascular disease, inflammatory bowel disease (IBD), and malignancies (Gaudino et al., 2021).

PCs in small intestine constitutively secrete HD5, HD6 and other antimicrobial proteins to protect the host against invading pathogens and to maintain commensal microbial communities (Al-Saffar, 2016). The clinical significance of PCs has been documented in Crohn's disease, which is characterized by PC dysfunction as evidenced by reduced HD5 production, alteration of resident microbiota and subsequent inflammation, an up-regulation of HD5 in colorectal mucosa has been observed in patients with HIV-1, possibly in response to intestinal inflammation (Hirao et al., 2014). Coeliac disease is associated with a reduction in the number of PCs in the small intestine of affected patients.

The other diseases which are associated with a reduction in the overall number of PCs in the epithelium of the intestine include malnutrition, parasitic infection and HIV/AIDS (Tobi et al., 2021). In some of the diseases which are associated with reduction of the average number of Paneth cells in the intestinal crypts, there is a concurrent depletion of PC, secretory granules and reduction of HD-5 immunoreactivity, on the other hand, diseases such as ulcerative colitis, tuberculous typhlitis and tumors of the GIT are associated with an increase in the number of Paneth cells (Iyer and Vaishnava, 2016, Lewin and Rouzioux, 2011, Sommers, 1966, Voshavar, 2019). The antimicrobial activity of α-defensins, combined with their effects on immune regulation and response, necessitates further investigation into the complex relationship between these peptides and HIV-1 pathogenesis (Dipankar Ghosh, 2000).

2.6 Mechanisms of action of Paneth cells in viral infections

Paneth cells are involved in the response to bacterial, viral, and parasitic GI tract infections since they are the key players in the innate immunity of the gut. Paneth cells prevent viral infections by using different mechanisms including anti-microbial products such as alpha-defensins, increasing IL-1β expression, increase in enteric α-defensin RNA levels and a decrease in α-defensin protein levels in Paneth cells macaques with SAIDS.

Alpha-defensins are potently anti-viral against both enveloped and non-enveloped viruses, the α-defensins inhibit fusion between enveloped viruses and cells by preventing interaction of virus glycoprotein with cell wall receptors (D'Agostino et al., 2009). On the other hand, α-defensins inhibit non-enveloped viruses by binding to and stabilizing their capsid, thereby disturbing the uncoating process (Llenado et al., 2009). Mouse adenovirus 2 infection is a natural pathogen of mice that infects the GIT. Since MAdV-2 is resistant to neutralization by α-defensins, it uses α-defensins to promote its growth in GIT (Salzman et al., 2010). In Mouse adenovirus 1 infections, α-defensins inhibits growth of virus. Paradoxically, MAdV-1 is inhibited by the same enteric α-defensins that enhance MAdV-2 infection (Salzman et al., 2010). Resistance to α-defensin neutralization and ability to exploit these host defense peptides to increase infection by MAdV-2 may be a consequence of evolution of this virus, particularly under selective pressure from abundant α-defensin secretion in mouse intestine (Deng et al., 2021). Human defensin 5 is a strong

inhibitor of a subset of human adenoviruses (HAdV), which cause diseases outside of GIT. The serotypes of HAdV are either resistant or enhanced by HD5 (Kelly et al., 2004).

Another case where barrier integrity is mediated by PCs is when the viral infection is compromised, in reduction of beneficial bacteria following HIV infection. Viral infection affects the integrity and function of epithelium of GIT (Garabedian et al., 1997, Lencer, 1998). Loss of integrity of intestinal epithelium following a viral infection is caused by increased IL-1β expression in PCs. The increased expression of IL-1β expression in PCs would suggest a possible mechanism whereby PCs respond to viral infection by secreting IL-1β, although they themselves have not been shown to be directly infected (Bevins and Salzman, 2011, Berkowitz et al., 2019).

A study conducted in 2010 found that Rhesus macaques with simian AIDS (SAIDS) due to chronic SIV infection had increased numbers of PCs per crypt but Paneth cells showed reduced numbers of cytoplasmic granules (Estes et al., 2010). This change is correlated with an increase in enteric α-defensin RNA levels and a decrease in α-defensin protein levels in Paneth cells, which was not observed in ileal loop model (Zaragoza et al., 2011). The authors proposed that PCs in macaques with SAIDS were undergoing high rates/levels of secretion, accounting for the absence of detectable α-defensins in PCs (Estes et al., 2010).

The loss of α-defensin in Paneth cells of macaques infected with SAIDS is with an increase in bacterial and eukaryotic infections of GI tract, suggesting that either defensins are ineffective against pathogens in context of SAIDS or that α-defensin protein synthesis is lost in SAIDS, resulting in reduced antimicrobial activity. Although SIV and HIV are not tropic for PCs, infection by these viruses influence their function (Zaragoza et al., 2011, Estes et al., 2010). Some viruses use Paneth cells products to enhance their growth in host or in other cases it is these Paneth cells products that help fight this infection. Therefore, Paneth cells play a crucial role in viral infection and its progression.

2.7 Combination Anti-Retroviral Drug (Atripla) Therapy and alcohol on the GIT

People living with HIV are more likely to use alcohol (Pandrea et al., 2010). In addition, alcohol abuse in HIV patients is associated with male gender, lower educational status and illicit drug use (Pandrea et al., 2010, Imhof et al., 2001). Many people who are diagnosed with HIV continue to drink alcohol despite their medical condition for a variety of reasons, including recreational

purposes and self-medication (Pandrea et al., 2010). Alcohol relaxes the brain and body, which can help relieve stress, encourage relaxation, and act as an appetite stimulant (Samet et al., 2007). Individuals living with HIV may be dealing with a significant amount of emotional distress and alcohol may provide temporary relief (Imhof et al., 2001). However, the combination of alcohol and ART can also alter mood and lead to numerous physical, psychological, and social problems (Pandrea et al., 2010). Incidentally, alcohol use and abuse occur simultaneously in individuals living with HIV/AIDS and have been linked to poor response to treatment as well as a more rapid progression of HIV disease (Samet et al., 2007). The underlying etiology of these effects is not well understood, one possible contributor is drug-drug interactions between alcohol and antiretroviral medications (ARV) (Iyer and Vaishnava, 2016).

Six distinct classes of ARV drugs are currently approved by the Food and Drug Administration (FDA) for the treatment of HIV-infected individuals. To ensure an effective therapy with lower risk of development of resistance of the HI virus, drugs from two or sometimes three classes are combined (Cihlar and Ray, 2010). In most cases HIV treatment is initiated with two drugs from the nucleoside/nucleotide reverse transcriptase inhibitors class combined with either an integrase inhibitor, non-nucleoside reverse transcriptase inhibitor or one protease inhibitor (Kallings, 2008). Nucleoside reverse transcriptase inhibitors (NRTIs), and nucleotide reverse transcriptase inhibitors (NtRTIs), often all referred to as NRTIs, work by targeting the action of an HIV protein called reverse transcriptase (Cihlar and Fordyce, 2016). Reverse transcription is a process were by reverse transcriptase coverts RNA into DNA after the HIV virus have released its genetic material into the host cell (Cihlar and Ray, 2010).

The reverse transcription process is ceased when NRTIs disrupt the construction of a new piece of pro-viral DNA and as a result HIV replication is stopped (Negin and Cumming, 2010). The combination of drugs in this regimen includes Abacavir, Emtricitabine, Lamivudine, Tenofovir disoproxil, Tenofovir alafenamide and Zidovudine (Cihlar and Fordyce, 2016). Non-nucleoside reverse transcriptase inhibitors (NNRTIs) also target reverse transcriptase enzyme, but in a different way to nucleoside reverse transcriptase inhibitors (NRTIs) (Cihlar and Ray, 2010). NNRTIs hinder the reverse transcriptase enzyme by binding directly to it, blocking the reverse transcription process (Cihlar and Fordyce, 2016). This regiment include Doravirine, Efavirenz, Etravirine, Nevirapine, Rilpivirine (Negin and Cumming, 2010).

The HIV integrase protein is vital for viral replication and is the main target of the integrase inhibitors (Cihlar and Ray, 2010). The integrase enzyme is responsible for inserting the viral genomic DNA into the host chromosome compliment (Cohen et al., 2011). The integrase enzyme binds to the host cell DNA, prepares a zone on the viral DNA for integration, and then transfers this processed strand into the host cell's genome (Cihlar and Fordyce, 2016). Integrase inhibitors prohibits the virus from inserting itself into the DNA of human cells (Cohen et al., 2011). C-C chemokine receptor type 5 (CCR5) is an example of an inhibitor that stops entry of the virus into the cell since HIV requires binding of its CD4 receptor and to a co-receptor for it to release its envelope, the CCR5 inhibitor bind to the co-receptor to blocks viral entry (Cihlar and Fordyce, 2016).

Protease inhibitors block the activity of the protease enzyme, which the HIV uses to break up large polyproteins into the smaller pieces required for assembly of new viral particles,booster drugs are used to 'boost' the effects of protease inhibitors(Mudgal et al., 2018). Adding a small dose of a booster drug to an antiretroviral treatment makes the liver break down the primary drug more slowly, which means that it stays in the body for longer times or at higher levels. Without the boosting agent, the prescribed dose of the primary drug would be ineffective (Cihlar and Fordyce, 2016).

Atripla is a daily fixed-dose combination tablet which contains Efavirenz, Emtricitabine, and Tenofovir that is used to treat HIV infection. It is used alone or with other HIV medications to help control HIV infection (Cohen et al.,2011). Efavirenz belongs to non-nucleoside reverse transcriptase inhibitors (NNRTIs) whereas emtricitabine and tenofovir belong to nucleoside reverse transcriptase inhibitors (NRTIs) group (Mudgal et al.,2018). Side effects of Atripla include diarrhea, nausea, and tiredness (Cohen et al.,2011).

Whether drug interactions between antiretroviral therapy (cART) medications and alcohol occur is unknown but based on the clinical pharmacology of alcohol and major classes of HIV therapeutics, there is a possibility of interactions of clinical significance (McCance-Katz, 2016). The principal metabolic route for alcohol is through alcohol dehydrogenase which mediates the conversion of alcohol to acetaldehyde in the liver (Cohen et al.,2011). Acetaldehyde is then converted to acetate by other enzymes and the final products in this metabolic pathway are carbon dioxide and water (McCance-Katz, 2016). Alcohol is also metabolized in the liver by the

cytochrome P450 (CYP 450) 2E1 and to a lesser extent by CYP 450 3A4 enzymes whose activity may be increased with chronic alcohol drinking (Negin and Cumming, 2010).

The two commonly used drugs in ART regiments have robust effects on CYP 450 3A4 drug metabolizing enzymes and are likely to affect both the pharmacokinetics and pharmacodynamics of alcohol. Ritonavir is an inhibitor of CYP 450 3A4 and it might potentially increase the effects of alcohol when these drugs are administered concomitantly (Imhof et al., 2001). Ritonavir is metabolized principally by CYP 3A4 and 2D6. Efavirenz is a potent inducer of CYP 3A4 which might decrease blood alcohol levels, potentially decreasing alcohol effects (Negin and Cumming, 2010). Efavirenz is principally metabolized by CYP 2B6 and CYP 3A4. Drug interactions might place patients at risk for toxicities or possibly for ineffective antiretroviral plasma concentrations, as well as for non-adherence to prescribed regimens (Imhof et al., 2001).

2.8 ARV drug metabolism and alcohol

Anti-retroviral drugs undergo significant metabolism in liver and small intestines, and there is substantial opportunity for alcohol to disrupt drug bioconversion in HIV patients, alcohol and other drugs are metabolized by the same enzymes that are involved in biotransformation of ARV drugs into toxic intermediates (McCance-Katz, 2016). These toxic compounds are further inactivated by phase 2 enzymes, such as glutathione S-transferase, N-acetyltransferases, sulfotransferases, UDP-glucuronosyltransferases, and methyltransferase (Llopis et al., 2016). Thus, HIV-infected patients who drink alcohol and are treated with ARV drugs are at risk of drug–drug interactions that may either decrease or inappropriately increase the effect of ARVs. For example, plasma concentration of ARV drug abacavir, which is extensively metabolized by alcohol dehydrogenase, increases up to 41 percent when taken concomitantly with alcohol (Imhof et al., 2001) Another potential consequence of drug–drug interactions is increased toxicity and development of liver damage in patients who already are at risk of developing liver disease because of direct toxicity of alcohol (Llopis et al., 2016).

The type of alcohol found in many alcoholic beverages induces activity of enzyme cytochrome P4503A4 CYP3A4 in liver both in vivo and in vitro (Monaco et al., 2016). This enzyme is responsible for metabolism and degradation of most of the drugs. Two types of ARV drugs the nonnucleoside reverse transcriptase inhibitors (NNRTIs), including delavirdine, nevirapine and

efavirenz, and PIs, such as ritonavir, nelfinavir, lopinavir, saquinavir, and indinavir are all susceptible to increased liver metabolism when taken together with alcohol, because of alcohol mediated induction of CYP3A4 enzyme system (McCance-Katz, 2016). Increased metabolism of ART components will result in sub-therapeutic drug levels in HIV patients who are abusing alcohol, and this could then lead to suboptimal viral control (Pandrea et al.,2010). This scenario is likely underestimated because routine monitoring of ARV levels is not common in HIV treatment settings (Llopis et al., 2016). The inconsistency of CYP3A4 activity already is greater in HIV patients than in uninfected control subjects, even in patients not receiving drugs that alter CYP3A4 activity (Monaco et al., 2016). Alcohol abuse by HIV infected individuals is a common and highly relevant factor capable of altering pharmacokinetics of ARVs (Bishehsari et al., 2017).

The response to ARV therapy is influenced by multiple viral, and host factors (Imhof et al., 2001). The combination of alcohol use and HIV treatment is not yet fully understood and is the subject of intense investigation (McCance-Katz et al.,2013). Alcohol may affect cART efficacy through diverse mechanisms, including decreasing patient adherence to treatment; altering liver function and ARV drug metabolism, alcohol may also accelerate liver disease in hepatitis C and B, which are frequent comorbidities in HIV-infected patients; by increasing viral replication or inducing immune activation, which may contribute to a poor ARV response (Pandrea et al.,2010).

2.9 The role Alcohol and Paneth cells in gastrointestinal inflammation

Gastrointestinal inflammation results from an inflammatory response caused by immune system against alcohol and its metabolites (Bishehsari et al., 2017). Alcohol can induce intestinal inflammation through a cascade of mechanisms that subsequently lead to general inflammation and organ dysfunction (Pandrea et al., 2010, Bishehsari et al., 2017). One of the mechanisms of action of alcohol is by increasing bacterial load and permeability of intestinal wall allowing bacteria to leak through. This affects mucosal immunity through the release of endotoxin (Zhou et al., 2020). Alcohol also affects mucosal immunity by suppressing PCs that secrete antibacterial compounds (Bishehsari et al., 2017).

Suppressed PCs secrete fewer antibacterial compounds, which can promote intestinal bacteria overgrowth and allow their byproducts such as endotoxins to enter through intestinal mucosal barrier (Iyer and Vaishnava, 2016). The bacteria, via endotoxins, trigger an inflammatory response

by intestine's immune system, causing a release of proinflammatory cytokines, the endotoxins and cytokines can then enter the liver directly interacting with hepatocytes and with immune active cells in the liver, causing local cytokine release that leads to fibrosis and causes additional inflammation (Bishehsari et al., 2017). The gut inflammation can also spread endotoxin and cytokines into bloodstream where they can enter central nervous system (CNS), causing neuroinflammation (Iyer and Vaishnava, 2016).

Alcohol can directly modulate both innate and adaptive immunity, further contributing to gut and gut-derived inflammation (Bishehsari et al., 2017, Samet et al., 2007, Bagasra et al., 1993). Alcohol suppresses gut immune system and reduces the ability of gut to clear harmful bacteria (Llopis et al., 2016); Imhof et al., 2001). Alcohol was found to affect intestinal mucosal immunity in so many ways including by reducing amount of anti-microbial molecules secreted by intestinal cells leading to bacterial overgrowth (Wang et al., 2016); suppressing the signaling molecule: interleukin-22, which negatively affects antimicrobial peptides (e.g., Reg3β and Reg3γ) and intestinal mucosal integrity (Wang et al., 2016); and suppressing signaling molecules and immune T-cells, thereby suppressing intestinal mucosal immune response and bacterial clearance (Bishehsari et al., 2017).

2.10 Aims and objectives

The study evaluated the histomorphometric changes in the small intestinal epithelium and paneth cells of male Sprague Dawley rats exposed to alcohol and/or combination anti-retroviral drug (Atripla) therapy (cART)

The objectives of this study were:

1. To evaluate the morphometric changes of crypts and villi dimensions in the jejunum and ileum.

2. To determine the location of the Paneth cells along the axis of the intestinal crypts of the jejunum and ileum.

3. To examine the histomorphological appearance of Paneth cells including their morphology and amounts of secretory granules, in the jejunum and ileum.

4. To examine the histomorphological appearance of stem cells in the crypts of the jejunum and ileum.

Chapter 3: MATERIALS AND METHODS

3.1 Introduction

The researcher conducted an experimental study, and this chapter clarifies methodology and rationale behind the research methods and techniques used in the study, including an elucidation of the study animals and design, histology, histology and immunohistochemical staining procedures, histomorphometric analysis and data analysis.

3.2 Study animals and design

The study utilized specimens of small intestines from 32 adult male Sprague-Dawley rats (Charles River Breeding Laboratory, Boston, MA, USA) at 10 weeks of age and weighing approximately 270g-320g donated from specimen bank maintained by researchers from previous studies in the School of Anatomical Sciences at University of the Witwatersrand. Ethical clearance to conduct the study was obtained from Animal Ethics Screening Committee (AESC) of University of the Witwatersrand (2018/011/58/C).

All animals were kept at Central Animal Services (CAS), University of the Witwatersrand, Johannesburg, Republic of South Africa under standard experimental conditions as approved by ASEC in line with international animal experimental ethics guidelines. The rats were housed in individual plastic cages (27 cages) that were 43mm long, 220mm wide and 200mm in height. The cages allowed free movement of rats and were maintained under standard animal house conditions of temperature of 21-23ºC and 12-hour light and dark cycle. All animals in the study were fed standard rodent diet and food and water were provided *ad libitum.*

The animals were divided into four groups (A –D) of 8 rats each (n=8) and were weighed weekly. Group A was treated with normal saline alone (normal chow and normal saline), Group B was treated with alcohol alone (normal chow and daily 10% v/v alcohol), Group C was treated with cART alone in gelatin cubes at a directly extrapolated human dose of 23.22 mgActive Ingrediate/kgBW/day , Group D was treated both alcohol (10% v/v ethanol) and cART at a dose of 23.22 mgAI/kgBW/day plus 10% v/v ethanol at *ad libitum*. All treatments lasted for 90 days.

The animals were terminated at the end of experiments (90 days) under pentobarbitone anesthesia (240mg/ml). The animals were then perfused at 2ml/min with saline 0.9% to flush out the blood from blood vessels. The specimens (GIT) were subsequently harvested and weighed and immediately fixed in 10% buffered formalin solution for further histological evaluation. All organs were immediately harvested, trimmed of connective tissue, dried on filter paper, weighed, and then fixed in appropriate fixative for further processing.

3.3 Histology

After fixation, GIT was stripped of mesentery using the Swiss roll technique (Al-Saffar, 2016). The small intestine was identified using landmarks and anatomical orientation. The stomach was first landmark identified as it was easy to identify through its anatomical morphology. According to revised guide for organ sampling and trimming in rats and mice, duodenum should be found 10mm distal to pyloric sphincter. Once duodenum was located; a colored paper pin was placed to make the landmark. A 100mm distance corresponds with length of duodenum in male Sprague-Dawley rats was measured distal to duodenum toward jejunum. The jejunum was located distal to 100mm distance as central section of small intestines. Between 45-55mm sections were taken from jejunum and pins were placed at both extremities of section. The cecum was used as a landmark to identify the ileum as ileum lies 1cm proximal to cecum. The ileum is shorter in length compared to jejunum, so a section of 25mm was taken.

A centimeter-long transverse and longitudinal sections were made from both jejunum and ileum sections placed in tissue cassettes and processed overnight in MYR ST-120-Casa Alvarez tissue processor. The tissue cassette first went through formalin, then through a series of graded concentrations of alcohol from 70% to 100% followed by xylene and lastly in wax. The tissues were embedded in paraffin wax on Leica EG1150 Tissue embedding center. Tissue blocks were sectioned at 4µm thick on Leica RM2125 RTS microtome in a 1 to 10 series of sections were obtained the 32 tissue blocks (i.e. 8 tissue blocks per group), giving a total of 320 tissue sections. Two consecutive sections from each group were mounted per slide for each of the stains utilized in the study. Therefore for uniform field of view for each stain, two consecutive tissue sections from each animal, per group (16 sections) were used for each of the stains. Thus, two sections from each animal at same level of section, from each group were stained with Hematoxylin and eosin (H & E), and similarly for Alcian Blue Periodic Acid-Schiff, Masson Trichrome, Anti-

Musashi-1 and Anti-alpha-defencin-5, ensuring that sections for each stain were obtained at same tissue level in all the treated animals in each group.

The section was picked up using Thermo Scientific Menzel –Glaser microscope slides and slides were air dried on a slide rack and then placed into incubator at 60 degrees to melt wax from slides. Sections were stained for hematoxylin and eosin, Alcian Blue, Periodic Acid-Schiff Masson's trichrome, anti-alpha defensin 5, and anti-Musashi-1. Hematoxylin and Eosin (H&E) stain was used to evaluate the general morphology of the small intestine, the ABPAS was used to visualize granules of PCs, Masson trichrome was used to visualize collagen content in muscular layer, anti-alpha-defencin-5 was used to immunohistochemically identify PCs and their secretory contents and anti-Musashi-1 was used to immunohistochemically localize intestinal stem cells.

3.4 Histology and immunohistochemical staining procedures.

Histological staining procedures for H&E (See appendix 4), ABPAS (See appendix 6) and Masson's trichrome (See appendix 5) were described following standard procedures published elsewhere (Feldman and Wolfe, 2014; Suvik and Effendy, 2012). Immunohistochemical staining protocols for anti-alpha defensin 5 (Porter et al., 1997; Sato et al., 2011; Wang et al., 2011), and anti-Musashi-1 (See appendix 7) (Barker et al., 2007; Chen et al., 2010; Dekaney et al., 2005) were adopted from previous publications on Sprague-Dawley rats' specimens (Bialkowska et al., 2016; Chen et al., 2010). Evaluation of H&E-stained segments of jejunum and ileum was carried out using ImageJ software. Brightfield microscopy (AxioScope, Zeiss, Oberkochen, Germany) at 10X was used to visualize H&E samples.

3.5 Histomorphometric analysis

3.5.1 Objective 1: To evaluate the morphometric changes of crypts and villi dimensions in the jejunum and ileum.

The morphometric changes of crypts and villi dimensions in the jejunum and ileum were evaluated by measuring and comparing the thickness of the walls of the small intestines, the number of villi, villus height and width as well as the number of crypts per complete section, crypt depth and width across the four groups

ImageJ software was used to measure wall thickness (WT), villous height (VH), villous width (VW), crypts depth (CD) and crypts width (CW) (Fig.1). At least 30 villi, crypts and muscular layer of small intestines were measured per animal, with eight animals in each group, yielding 960 measurements per group. Villi were chosen for measurement when intact from crypt-villus junction to another crypt-villus junction and central lacteal present. The crypts were measured if intact on both side of crypt-villus junction.

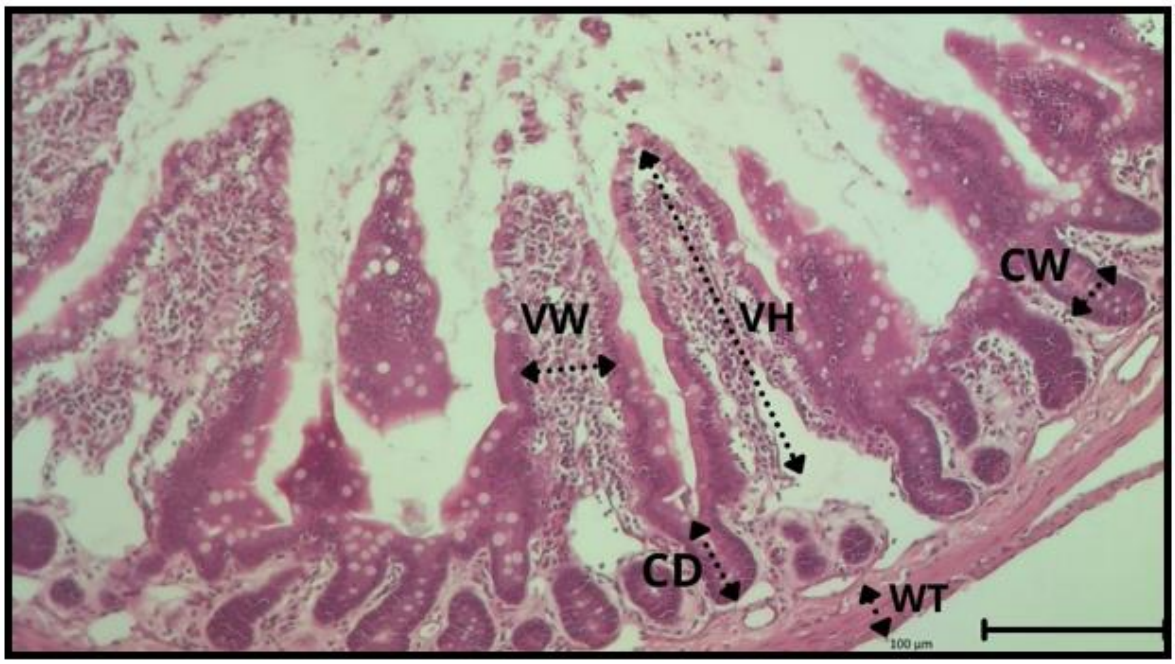

Figure 1. The photomicrograph shows an H&E-stained section of Sprague-Dawley rats' small intestine segment at 10x objective that depicts the method of measurement of chosen parameters. Abbreviations: WT=wall thickness, CD=crypts depth, VW=villous width, VH=villous height and CW=crypts width. Scale bar=100µm.

3.5.2 Objective 2: To determine the location of the Paneth cells along the axis of the intestinal crypts of the jejunum and ileum.

The location of Paneth cells along the axis of the intestinal crypts of the jejunum and ileum were determined by presence and position along the axis

3.5.3 objective 3: To examine the histomorphological appearance of Paneth cells including their morphology and amounts of secretory granules, in the jejunum and ileum.

The histomorphological appearance of Paneth cells including their morphology and amounts of secretory granules, in the jejunum and ileum was examined by measuring Paneth cell density, morphology, number, the existence of granules and their intensity of granular staining using Linkert's scale.

Four photomicrographs were taken from each slide of jejunum and ileum, using systemic sampling method, moving in one direction from bottom to top of slide to avoid duplicating same area of slide twice. Five photomicrographs were taken from each animal per group giving and therefore a total of 40 pictures were obtained per group (5 x 8) to determine presence and location of PCs using ABPAS. The crypts which had PCs were divided into zones according to a previous publication (Al-Saffar, 2016). The first zone was zone 1 being the base of crypts, zone 2 being the proliferation zone, zone 3 being the differentiation zone (Fig.2)**.** A standardized rating system was also used for each zone to score the zones based on the density of PCs and the concentration of their granules. score of 0=No Paneth cells present, score of 1=low Paneth cell presence, Score of 2= medium Paneth cells presence, and score of 3= high Paneth cells presence. For Paneth cells granules stimulation, 1= 25% Paneth cells granule stimulation. 2= 50% Paneth cells granules stimulation. 3= 75% Paneth cell granule stimulation. 4=Paneth cell present with 100% Paneth cells granules stimulation.

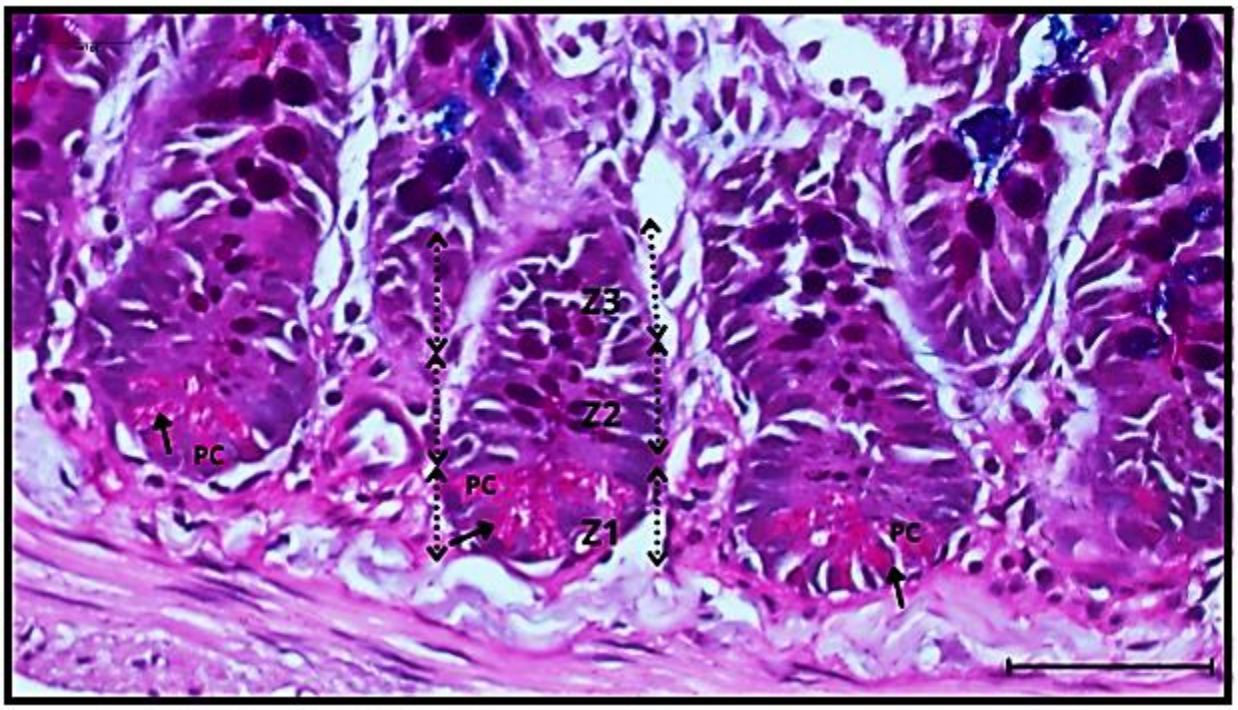

Figure 2. The photomicrograph shows an ABPAS-stained section of Sprague-Dawley rats' small intestine segment at 40x objective that illustrates the intestinal crypts differentiated into zones from base of crypts up to crypt-villus junction to show specific location of Paneth cells and Paneth cells granules (black arrows). Abbreviations: PC=Paneth cells Z1= zone 1 (basement zone), Z2= zone 2 (proliferation zone), Z3=zone 3 (differentiation zone), Scale bar=20µm.

3.5.4 Objective 4: To examine the histomorphological appearance of intestinal stem cells (ISC) in the crypts of the jejunum and ileum.

The histomorphological appearance of stem cells in the crypts of the jejunum and ileum were examined by locating and counting the number of stem cells per crypts. This was done using Masson's trichrome, anti-alpha defensin 5, anti-Musashi-1.

The Masson trichrome stain was used to demonstrate collagen and smooth muscles. The collagen content was quantified using stain since it stains collagen green. Image J was used to measure area-stained green for quantification of amount of collagen. This was achieved by separating red, green blue (RGB) channels on ImageJ and selecting green, then a threshold was made which only picked up green. The region which contained collagen in each of five photomicrographs per animal was measured and values were summed up to get total collagen content in each animal. The mean collagen content was calculated for each group and a graph plotted. A standardized rating system was conducted to determine any non-pyramidal morphological variation in PCs because of treatment. 0=No Paneth cells present, 1=normal pyramidal Paneth cells present, 2=normal pyramidal Paneth cells present+ non-pyramidal Paneth cells present, 3=only non-pyramidal Paneth cells present.

Further analysis of cell count was done for number of Paneth cells and five microphotographs were taken for purpose of counting number of Paneth cells in each picture. The final number of Paneth cells was divided by total number from 8 animals in each group. The mean number of paneth cells in each group was subsequently determined. For quantification of number of secretory granules of Paneth cells and anti-Musashi-1antibody, ImageJ software was used. The 3,3'-diaminobenzidine was used as the quantification reference on slides with hematoxylin counterstain. The images were analysed under quantification units of intensity. The intensity numbers were then converted into optical density (OD) by using formula OD=log (max intensity/mean intensity). Subsequently, image intensity was quantified based on average darkness of images due to DAB signal. A graph

was plotted to see which group produced highest intensity with 0-1 being low intensity, 1-2 being medium, 2-3 being high and greater than 3 being very high intensity following measurement of OD.

3.6 Data analysis

Data was exported from ImageJ software onto an excel spreadsheet (Microsoft excel 2016). Data was then exported into STATA SE 15 (4905 Lakeway Drive, College Station, TX, USA). Categorical data was presented as numbers and percentages. Continuous data was presented as means and standard deviation (SD). Data on counts and measurements was expressed as frequency tables. Normality test was done using Shapiro–Wilk W test. Comparison of means between groups of experimental and/or control animals was done using ANOVA followed by Bonferroni tests.

Chapter 4: RESULTS

4.1 Introduction

In this chapter, attention is paid to data analysis and interpretation. Results from histological staining for H&E, ABPAS, Masson trichrome, immunohistochemical staining protocols for anti-alpha-defencin-5, and anti-Musashi-1 are reported.

4.2.1Morphometric changes of the crypts and villi dimensions in the jejunum

The sections of specimens from control animals (Group A- saline treated animals) showed well-preserved epithelial architecture; villi were tongue-shaped and longer, while crypts were deeper with normal muscular layer (Fig.3A.). In the mucosa of Group B (alcohol only treated animals) most of the villi are poorly developed as evidenced by villous blunting, atrophy, reduced crypt-depth and disruption of muscular wall (Fig.3B). Findings from animals in Group C (cART only treated animals) included atrophic villi, reduction of depth of intestinal crypts and thickening of muscular wall (Fig.3C). The villi in animals from Group D (cART+ alcohol treated animals) were stripped of cells and all essential layers, the number of crypts were reduced, and muscular layer was atrophic. In some areas, crypts disappeared (Fig.3D).

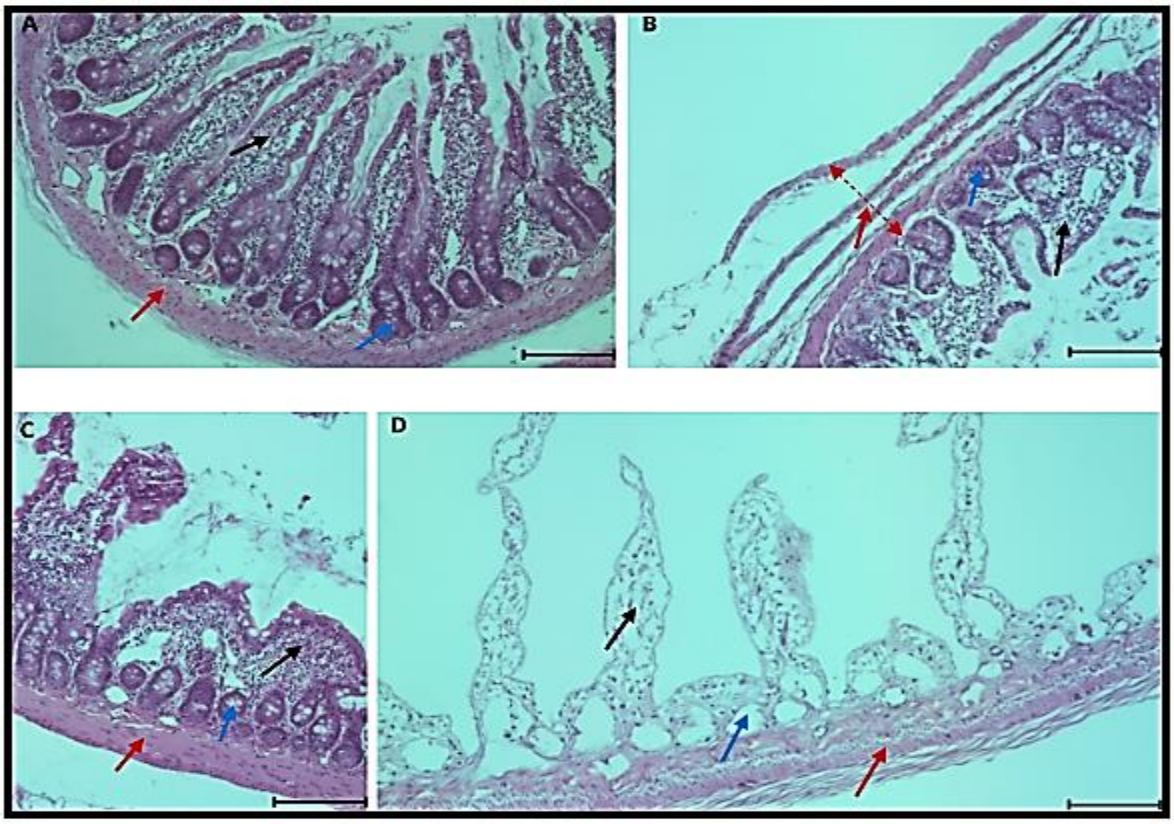

Figure 3. The photomicrograph shows the mucosa of the jejunum at 10x objective stained with H&E depicting normal tall villi (black arrow), with deep crypts (blue arrow) and normal muscular layer (red arrow) **A,** blunting of the villi (black arrow), the crypts are shallower (blue arrow), disruption of the muscular wall (red arrow) **B**, atrophic villi (black arrow), shallow crypts and thick muscular wall (red arrow) **C**, villous stripping (black arrow), crypts disappearance (blue arrow) and atrophy of the muscular wall (red arrow) **D**. Scale bar=100µm.

4.2.2 Morphometrics of intestinal parameters in jejunum

The parameters such as number of villi and crypts, height and width of villi, depth and width of crypts and thickness of muscular layer were all measured to determine any morphometric changes in jejunum of small intestine segments of Sprague-Dawley rats.

There was an increase in number of villi in jejunum between control group and experimental animals, with the mean number of villi as follows: Group A (control) = 20±3.78µm, Group B (Alcohol) was 27±1.97µm, Group C (Combination Anti-Retroviral Therapy) was 42±2.31µm and Group D (Alcohol+ Combination Anti-Retroviral Therapy) was 42±1.95µm. There was a

statistically significant difference in number of villi between Group A and Group B; Group A and Group C; Group B and Group D; Group C and Group D ($p<0.05$) (Fig.4A). The difference in mean number of crypts in animals of Group C and Group D was also statistically significant ($p<0.05$) (Fig.4B). Additionally, the difference of mean height of villi in Group B and Group D and, between Group C and D was statistically significant ($p<0.05$) (Fig.5A). The mean width of the villi in Group B was 109±14.57µm, Group C 61±9.37µm and Group D 61±10.71µm. The difference in mean height across groups was statistically significant ($p<0.05$) (Fig.5B) Groups compared as follows (Table 1).

The mean depth of crypts in jejunum segment of small intestine in Group C was 57±8.88µm whereas for Group A was 247±17.65µm. The difference in mean depth of crypts in both Group A and Group B and, Group A and Group C was statistically significant ($p<0.05$) (Fig.6A). There was an increase in width of crypts in all experimental animals, with there being a statistically significant difference between Group A and Group B and, Group A and Group C ($p<0.05$) (Fig.6B). The mean thickness of muscular layer for Group B was 160±6.47µm and for Group A it was 139±4.56µm. The difference in mean thickness of muscular layer for the animals in Group A and Group D, Group B and Group D and, Group C and Group D were all statistically significant ($p<0.05$) (Fig.7A and Table 1).

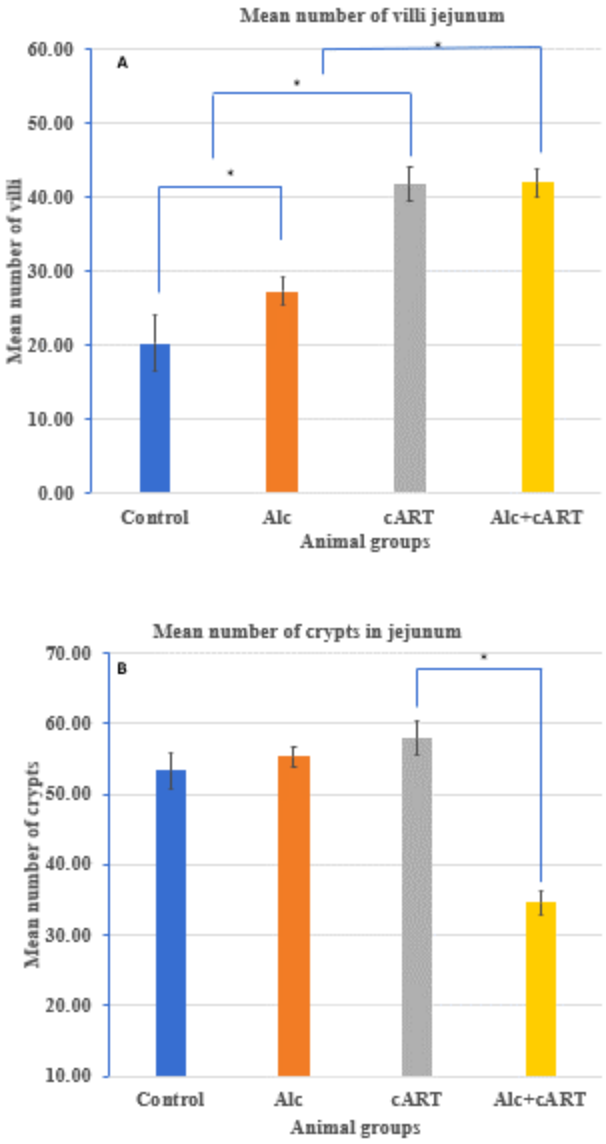

Figure 4. The effect of alcohol and/or cART therapy on the jejunum of the Sprague-Dawley rats after 13-week treatment period. (A) the number of villi. (B) the number of crypts. Bars indicate the mean±SD. Control group (Group A), Alcohol (Group B), Combination Anti-Retroviral Therapy (Group C) and Alcohol+ Combination Anti-Retroviral Therapy (Group D).

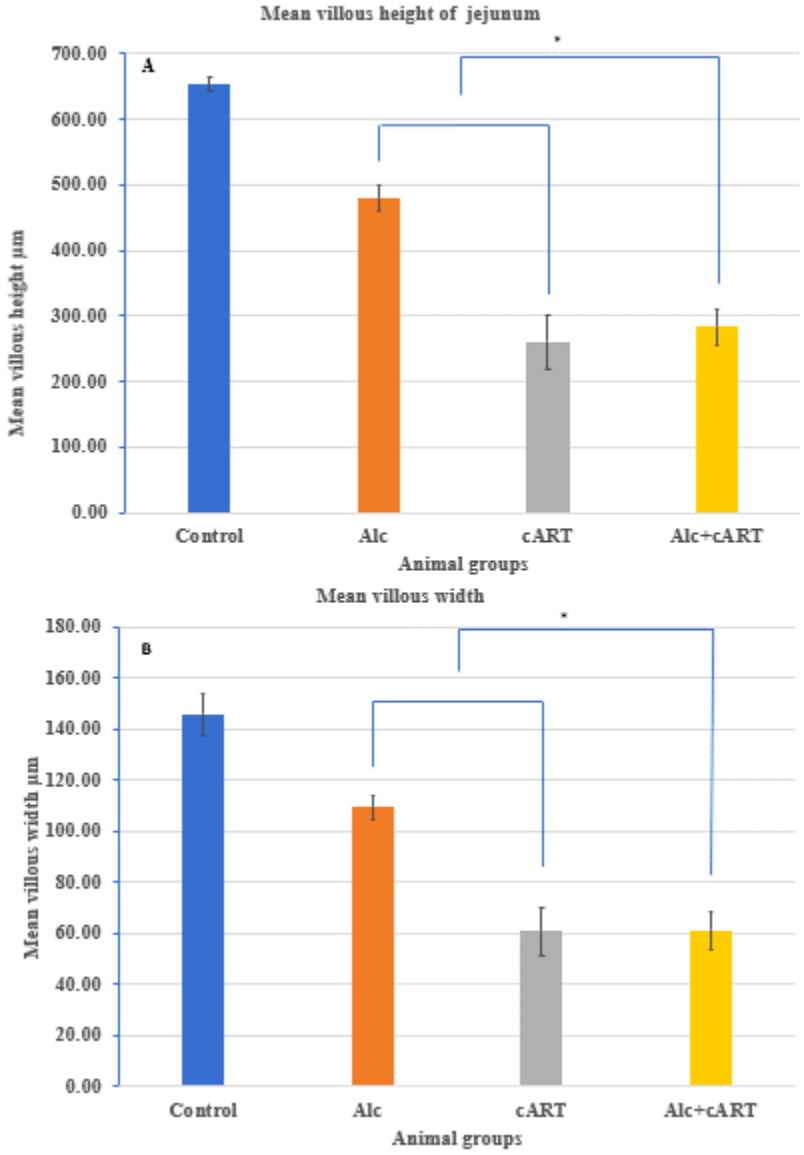

Figure 5. The effect of alcohol and/or cART therapy on the jejunum of the Sprague-Dawley rats after 13-week treatment period. (A) villous height. (B) villous width. Bars indicate the mean±SD. Control group (Group A), Alcohol (Group B), Combination Anti-Retroviral Therapy (Group C) and Alcohol+ Combination Anti-Retroviral Therapy (Group D).

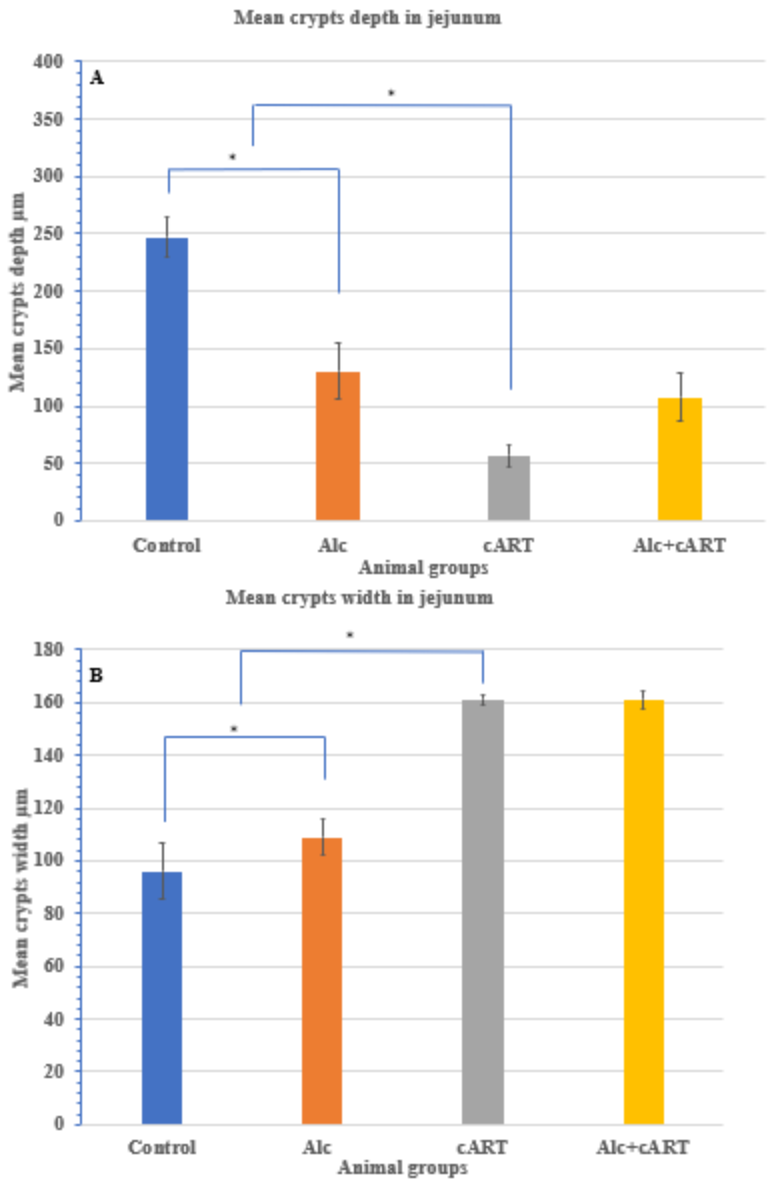

Figure 6. The effect of alcohol and/or cART therapy on the jejunum of the Sprague-Dawley rats after 13-week treatment period. (A) crypts depth. (B) crypts width. Bars indicate the mean±SD. Control group (Group A), Alcohol (Group B), Combination Anti-Retroviral Therapy (Group C) and Alcohol+ Combination Anti-Retroviral Therapy (Group D).

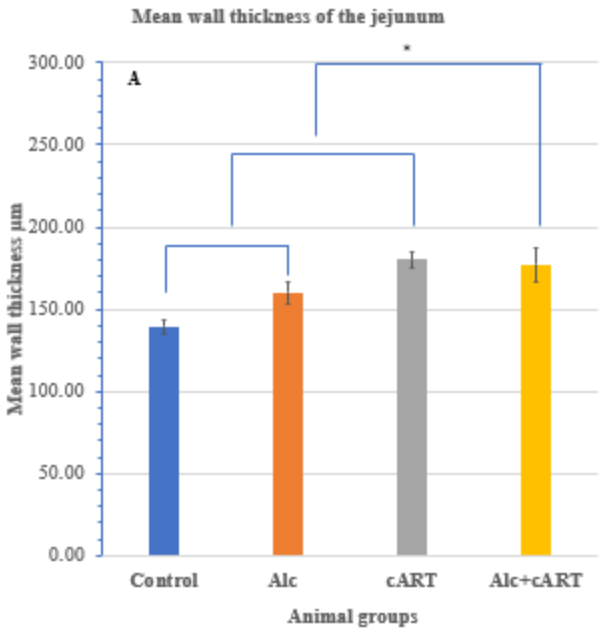

Figure 7. The effect of alcohol and/or cART therapy on the jejunum of the Sprague-Dawley rats after 13-week treatment period. Wall thickness (G). Bars indicate the mean±SD. Control group (Group A), Alcohol (Group B), Combination Anti-Retroviral Therapy (Group C) and Alcohol+ Combination Anti-Retroviral Therapy (Group D).

4.2.3 Morphometric changes of the crypts and villi dimensions in the ileum

The ileum of Group A animals showed well preserved epithelial architecture, villi are short and fewer. The crypts are shallower with normal thinner muscular layer (Fig.8A). Majority of villi in Group B animals are poorly developed and are stripped of all layers and cells. Furthermore, crypts of animals in Group B were damaged. In some areas crypts were not visualized, and muscular wall has been disrupted (Fig.8B). The intestinal section of Group C villi is atrophic with removal of the essential layers, crypts are destroyed, and muscular wall is thick (Fig.8C). The villi of small intestines of Group D animals have been stripped of cells and being curved in, crypts are proliferating, and muscular layer has enlarged (Fig.8D).

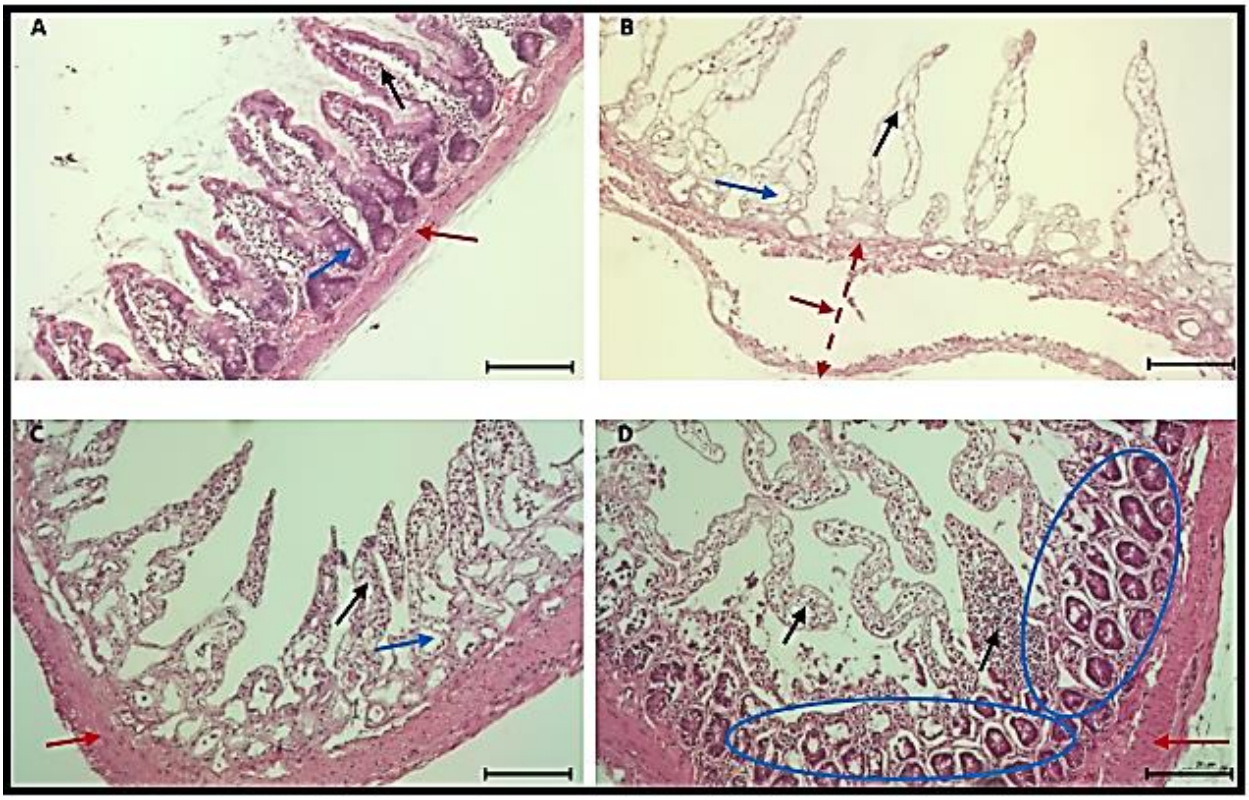

Figure 8. The photomicrograph s shows the mucosa of the ileum at 10x objective stained with H&E illustrating normal short villi (black arrow), with shallow crypts (blue arrow) and normal thin muscular layer (red arrow). **A,** there is villous stripping (black arrow), crypts disappearance (blue arrow), disruption of the muscular wall (red arrow). **B**, atrophic villi (black arrow), crypts disappearance (blue arrow) and thick muscular wall (red arrow) **C**, villous eroding, and curving (black arrow), proliferation (blue arrow) and atrophy of the muscular wall (red arrow) **D**. Scale bar=100µm.

4.2.4 Morphometrics of intestinal parameters in ileum

There was an increase in the number of villi in ileum between control group and experimental animals, with mean number of villi as follows: Group A (control) = 13±1.18 µm, Group B (Alcohol) was 13±1.29µm, Group C (Combination Anti-Retroviral Therapy) was 38±4.31µm and Group D (Alcohol+ Combination Anti-Retroviral Therapy) was 38±1.97µm. There was statistically significant difference in mean number of villi between Group A and Group C ($p<0.05$), and Group B and Group D ($p<0.05$) (Fig.9A). The difference in the mean number of crypts in animals in Group A and Group B was also statistically significant ($p<0.05$) and similarly, Group C and Group D ($p<0.05$) (Fig.9B). The difference of mean height of villi in Group B, and Group D and the control group was statistically significant ($p<0.05$) (Fig.10A). The mean width of villi with Group D was 130±10.75µm as compared to 184±18.32µm for Group A, and the difference was statistically significant ($p<0.05$) (Fig.10B and Table 1).

The mean depth of crypts of ileum in animals in Group C was 58±10.25µm whereas Group A was 279 ±8.21µm (Fig.11A). The difference in mean depth of crypts in Group A and all experimental groups was statistically significant ($p<0.05$) (Fig.11A). There was a statistically significant difference in mean width of crypts between Group B and Group C, and Group C and Group D ($p<0.05$) (Fig.11B). The mean thickness of muscular layer for Group A was 146±8.80µm, for Group B was 185±1.31µm, for Group C was 183±14.22µm and Group D was 199±4.95µm. The difference in mean thickness of muscular layer for animals in Group A and Group B; Group A and Group C; Group A and Group D were statistically significant ($p<0.05$) (Fig.12A and Table 1)

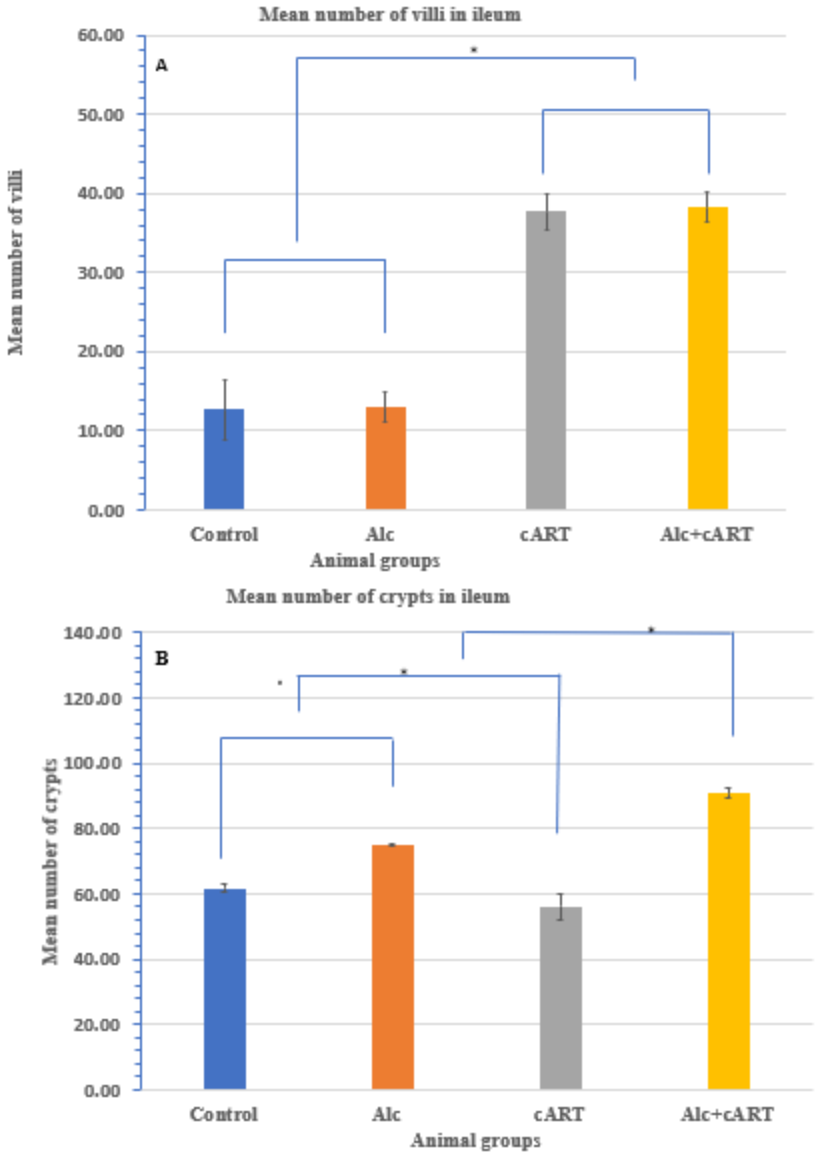

Figure 9. The effect of alcohol and/or cART therapy on the ileum of the Sprague-Dawley rats after 13-week treatment period. (A) the number of villi. (B) the number of crypts. Bars indicate the mean±SD. Control group (Group A), Alcohol (Group B), Combination Anti-Retroviral Therapy (Group C) and Alcohol+ Combination Anti-Retroviral Therapy (Group D).

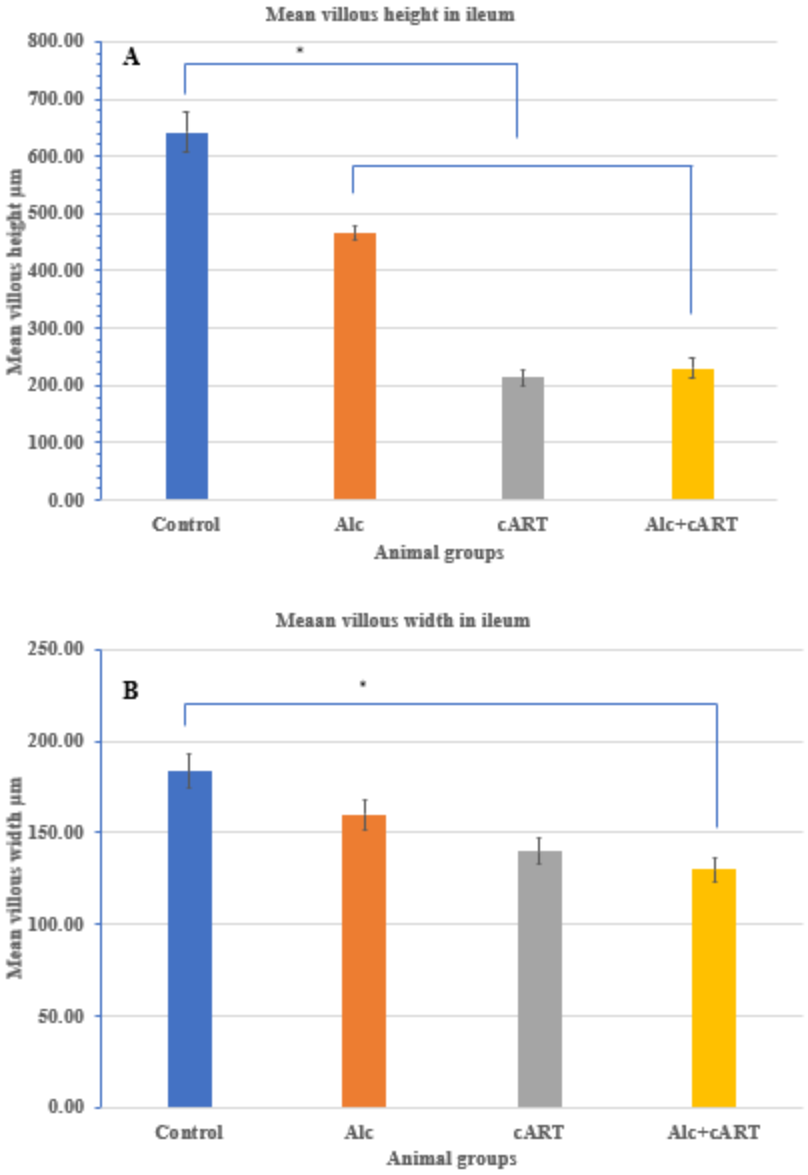

Figure 10. The effect of alcohol and/or cART therapy on the ileum of the Sprague-Dawley rats after 13-week treatment period. (A) villous height. (B) villous width. Bars indicate the mean±SD. Control group (Group A), Alcohol (Group B), Combination Anti-Retroviral Therapy (Group C) and Alcohol+ Combination Anti-Retroviral Therapy (Group D).

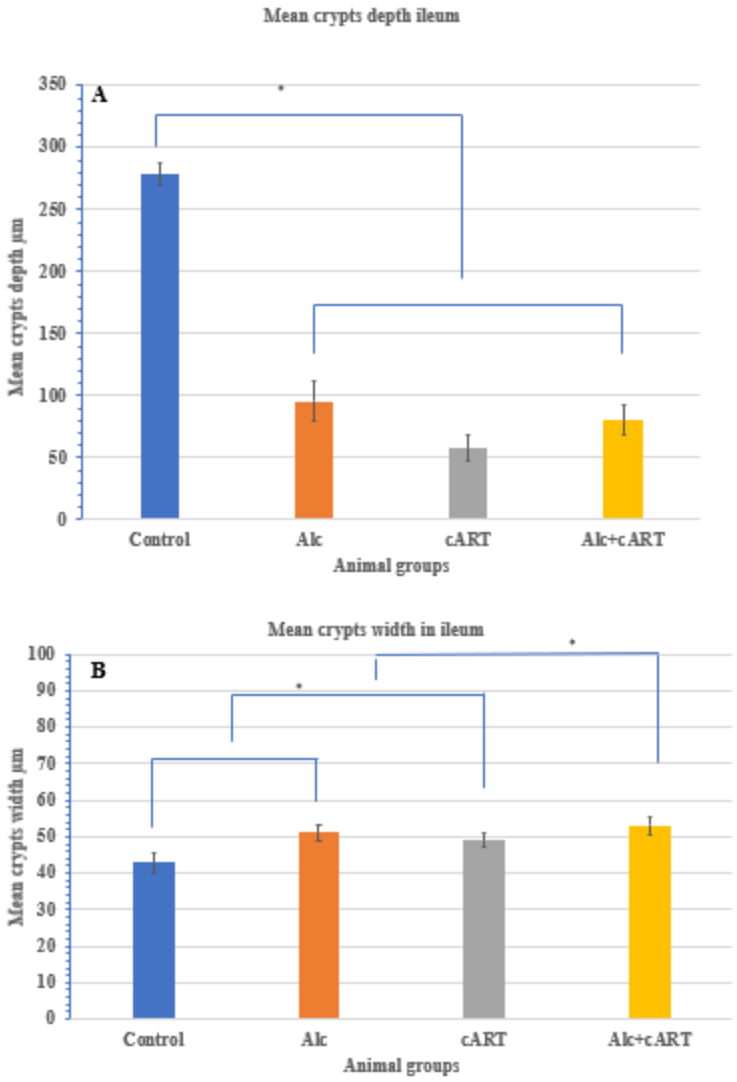

Figure 11. The effect of alcohol and/or cART therapy on the ileum of the Sprague-Dawley rats after 13-week treatment period. (A) crypts depth. (B) crypts width. Bars indicate the mean±SD. Control group (Group A), Alcohol (Group B), Combination Anti-Retroviral Therapy (Group C) and Alcohol+ Combination Anti-Retroviral Therapy (Group D).

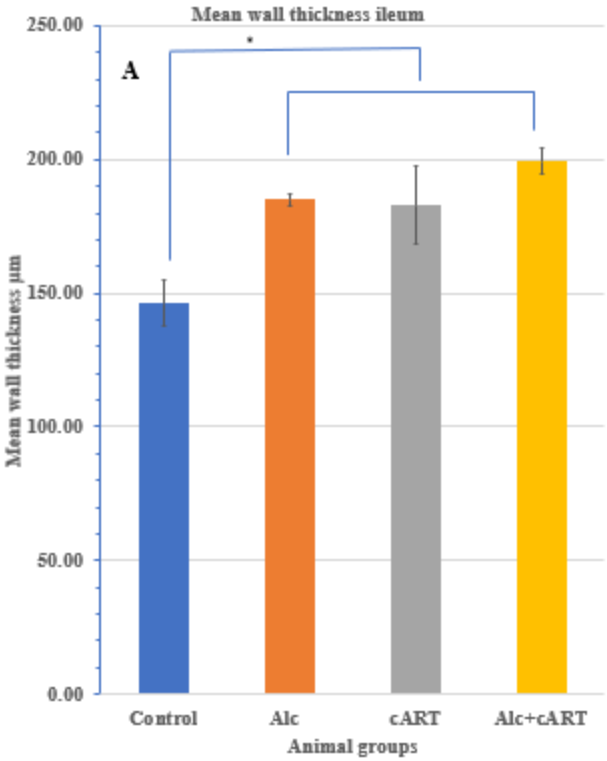

Figure 12. The effect of alcohol and/or cART therapy on the jejunum of the Sprague-Dawley rats after 13-week treatment period. Wall thickness (G). Bars indicate the mean±SD. Control group (Group A), Alcohol (Group B), Combination Anti-Retroviral Therapy (Group C) and Alcohol+ Combination Anti-Retroviral Therapy (Group D).

Table 1. The differences in the means of the Groups compared for the jejunum and ileum

	Jejunum	**Ileum**
Differences between	**P value**	**P value**
Mean number of villi		
Group D and C	0.01**	0.00**
Group D and B	0.01**	0.00**
Group D and A	0.13*	0.48*
Group C and B	0.47*	0.45*
Group C and A	0.00**	0.02**
Group B and A	0.00**	0.01**
Mean number of crypts		
Group D and C	0.02**	0.01**
Group D and B	0.37*	0.06*
Group D and A	0.27*	0.00**
Group C and B	0.09*	0.14*
Group C and A	0.09*	0.12*
Group B and A	0.44*	0.41*
Mean villous Height		
Group D and C	0.02**	0.00**
Group D and B	0.01**	0.00**
Group D and A	0.08*	0.04**
Group C and B	0.14*	0.30*
Group C and A	0.39*	0.01**
Group B and A	0.45*	0.01**
Mean villous width		
Group D and C	0.01**	0.00**
Group D and B	0.00**	0.00**
Group D and A	0.05*	0.09*
Group C and B	0.33*	0.08*
Group C and A	0.42*	0.02**
Group B and A	0.48*	0.02**
Mean crypts depth		
Group D and C	0.28*	0.35*
Group D and B	0.05*	0.18*
Group D and A	0.06*	0.00**
Group C and B	0.01**	0.22*
Group C and A	0.05*	0.00**
Group B and A	0.02**	0.00**
Mean crypts width		
Group D and C	0.05*	0.07*
Group D and B	0.06*	0.05*
Group D and A	0.13*	0.38*
Group C and B	0.44*	0.30*

Group C and A	0.04**	0.14*
Group B and A	0.03**	0.12*
Mean wall thickness		
Group D and C	0.01**	0.00**
Group D and B	0.01**	0.00**
Group D and A	0.01**	0.02**
Group C and B	0.34*	0.13*
Group C and A	0.18*	0.00**
Group B and A	0.28*	0.00**

**P value <0.05 statistically significant

*P value >0.05 NOT statistically significant

4.3.1The location of Paneth cells along the axis of intestinal crypts of jejunum

The sections of the specimens from control animals (Group A- saline treated animals) showed a normal presentation of PCs located near the basement membrane in the base of crypts and their granules unstimulated staining pale magenta in colour (Fig.13A.). In the mucosa of Group B (alcohol only treated animals) there was a low density of PCs in the base of crypts, but a high amount of stimulated Paneth cells granules as evidenced by increased staining intensity (magenta pink) (Fig.13B). Findings from animals in Group C (cART only treated animals) included reduction of PCs density in base of the crypts and unstimulated PCs granules (Fig.13C). The PCs in animals from Group D (cART+ alcohol treated animals) were located both in the base of crypts (zone 1) and proliferation zone (zone 2). PCs in both zones showed highly stimulated PCs (magenta pink) (Fig.13D).

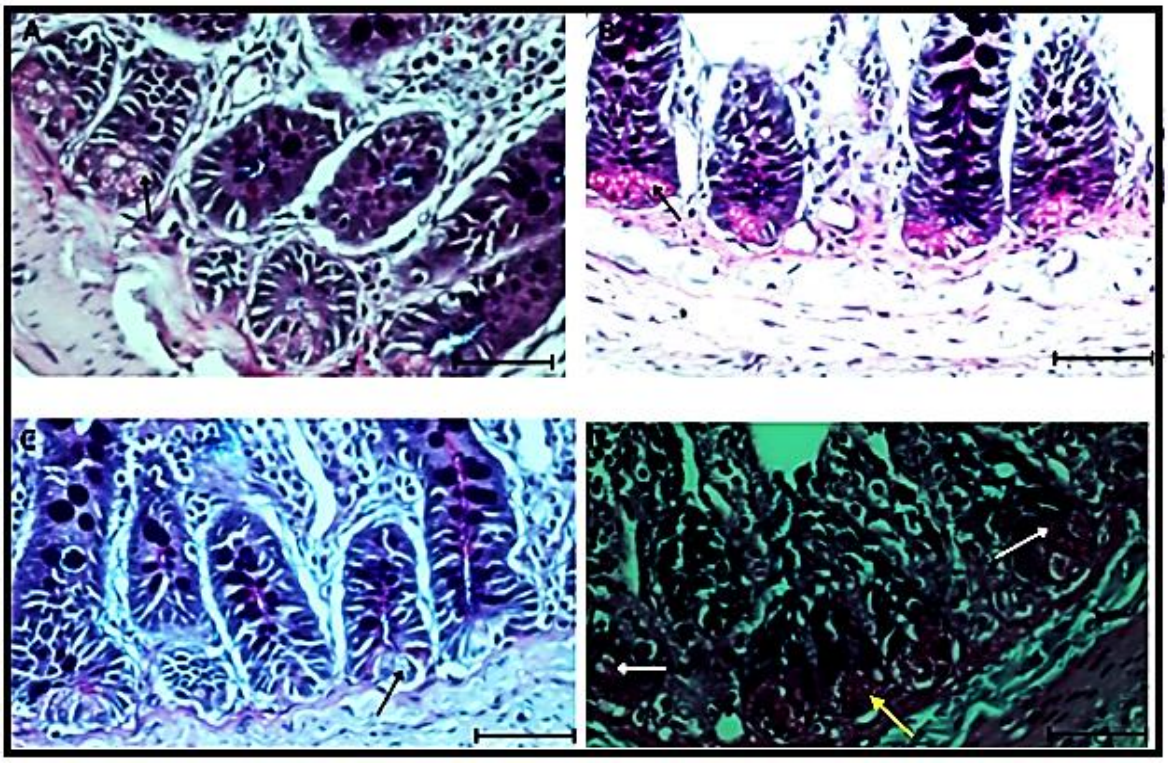

Figure 13. The photomicrograph shows the mucosa of the jejunum stained with ABPAS illustrating a high density of PCs in the base of the crypts with 25% of granules stimulated (black arrow) **A,** a low density of PCs in the base of the crypts with 75% of granules being stimulation (black arrow) **B**, a low density of PCs located in the base of the crypts (black arrow) and 25% of granules show stimulation (black arrow) **C**, PCs located in the base of the crypt (black arrow) and the proliferation zone (white arrow) with 100% granules stimulation (yellow arrow) **D**. Scale bar=20µm.

4.3.2 Morphometrics associated with Paneth cells in jejunum

Group A to Group C Paneth cells were all located in zone 1, Group D Paneth cells were in zone 1 and zone 2 (Fig.14). There was a decrease in Paneth cell density, Group A scored 3±0.18, Group B scored 1±0.4, Group C scored 2±0.1 and Group D scored 2±0.1 and in zone 2 Group D scored 1±0.12 (Fig.14A). There was statistically significant difference in mean score of Paneth cell density between Group D in zone 1 and Group D in zone 2 ($p<0.05$), (Fig.14A). There was a high stimulation of Paneth cells granules in Group D in both zone1 and zone 2 with a score of 4±0.72 and 2.5±0.07 with differences in means being statistically significant ($p<0.05$) (Fig.14B)

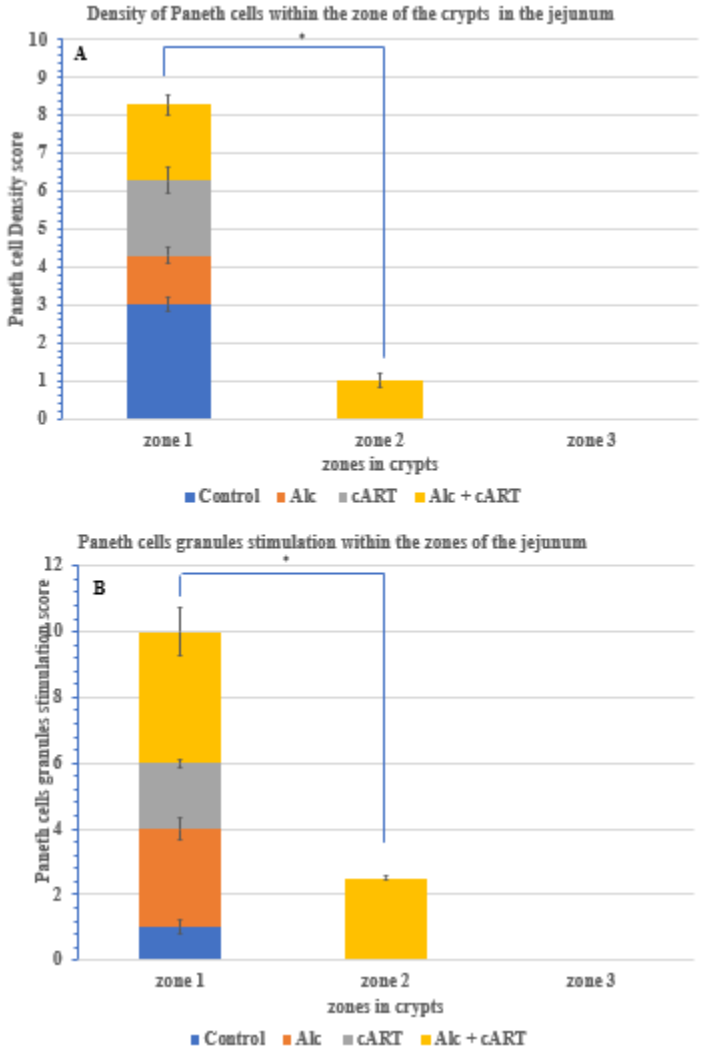

Figure 14. The effect of alcohol and/or cART therapy on the location of Paneth cells in the jejunum of the Sprague-Dawley rats after 13-week treatment period. (A) Density of Paneth cells within the zones of the intestinal crypts. (B) Paneth cells granules stimulation within the zones of the intestinal crypts. Bars indicate the mean±SD. Control group (Group A), Alcohol (Group B), Combination Anti-Retroviral Therapy (Group C) and Alcohol+ Combination Anti-Retroviral Therapy (Group D).

4.3.3 The location of Paneth cells along the axis of intestinal crypts of ileum

Sections from ileum of Group A animals showed PCs resting on the base of crypts with unstimulated granules (Fig.15A.). A medium density of PCs was located at the base of crypts in Group B. A large proportion of their granules (75%) were stimulated as evidenced by deep intensity of ABPAS stain (Fig.15B). In Group C, PCs were located at the base of the crypts with moderate granules stimulated (Fig.15C). The PCs in Group D animals were found in high density in both proliferation and basal zones. In addition, Paneth cells of both zones showed increased densities of stimulated granules when compared to other groups (Fig.15D).

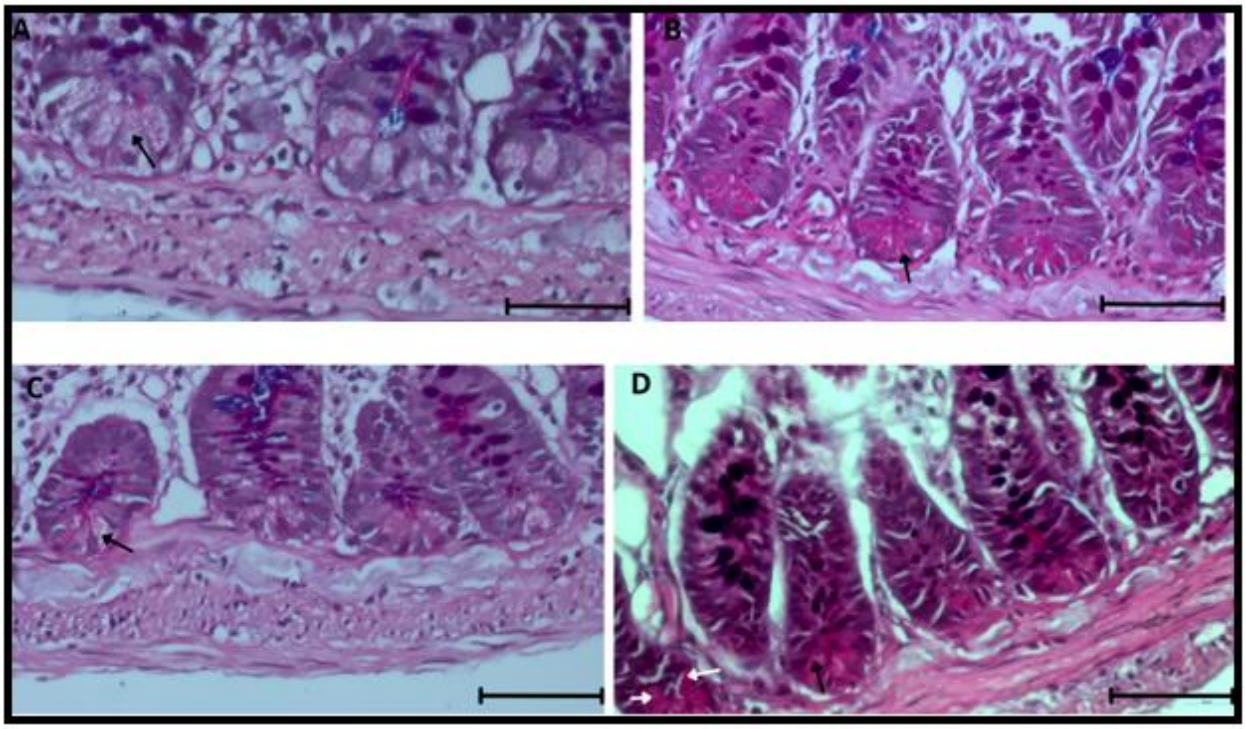

Figure 15. The photomicrograph shows the mucosa of the ileum stained with ABPAS illustrating a high density of PCs in the base of the crypts with 25% of their granules stimulated (black arrow) **A,** medium density of PCs in the base of the crypts with 75% of granules being stimulated (black arrow) **B**, low density of PCs located in the base of the crypts (black arrow) with 50% of granules stimulated (black arrow) **C**, a high density of PCs located both in the basal (black arrow) and the proliferation zones (white arrow) showing 100% granule stimulation (black arrow) **D**. Scale bar=20µm.

4.3.4 **Morphometrics associated with Paneth cells in ileum.**

From Group A to Group C animal groups, PCs were located exclusively in base of intestinal crypts (zone 1 region), but in Group D, PCs were found in both base and proliferative regions (zone 1 and zone 2) of intestinal crypts (Fig.16A and B). There was a decrease in density of PCs in Group B in zone 1 region and Group D in zones 1 and 2. There was statistically significant difference in mean score of PCs presence between Group D in zone 1 and Group D in zone 2 ($p<0.05$), (Fig.16A). There was a high stimulation of Paneth cells granules in Group D both in zone1 and zone 2 with a score of 4±0.72 and 2±0.29 with differences in means being statistically significant ($p<0.05$) (Fig.16B).

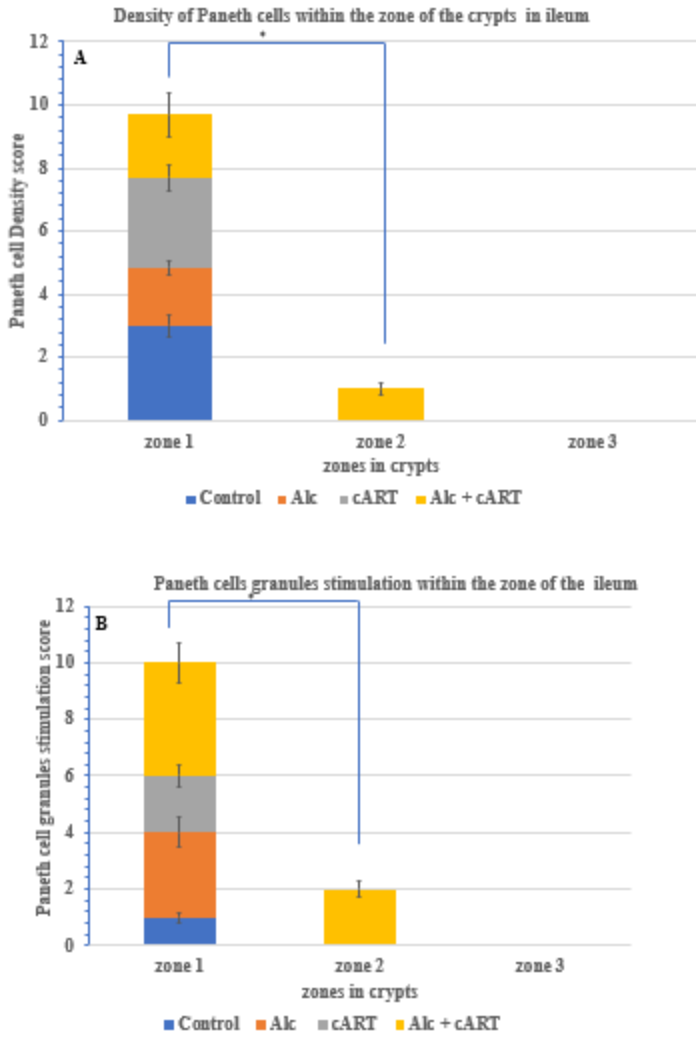

Figure 16. The effect of alcohol and/or cART therapy on the location of Paneth cells in the ileum of the Sprague-Dawley rats after 13-week treatment period. (A) Density of Paneth cells within the zones of the intestinal crypts. (B) Paneth cells granules stimulation within the zones of the intestinal crypts. Bars indicate the mean±SD. Control group (Group A), Alcohol (Group B), Combination Anti-Retroviral Therapy (Group C) and Alcohol+ Combination Anti-Retroviral Therapy (Group D).

4.4.1 Collagen content in the wall of the jejunum segment of small intestines

The control animals (Group A- saline treated animals) showed well-preserved mucosal epithelial architecture with normal amount of collagen content and muscular wall thickness (Fig.17A). In mucosa of Group B (alcohol only treated animals) there was atrophic villi and degenerated crypts with increased collagen in proportion with submucosa and muscularis externa (Fig.17B). Findings from animals in Group C (cART only treated animals) showed reduced thickness of muscularis externa and a low density of collagen fibers in same layer (Fig.17C). There was a marked increase in density of collagen fibers in animals from Group D (cART+ alcohol treated animals) this was also proportional with overall increase in the thickness of muscularis externa (Fig.17D).

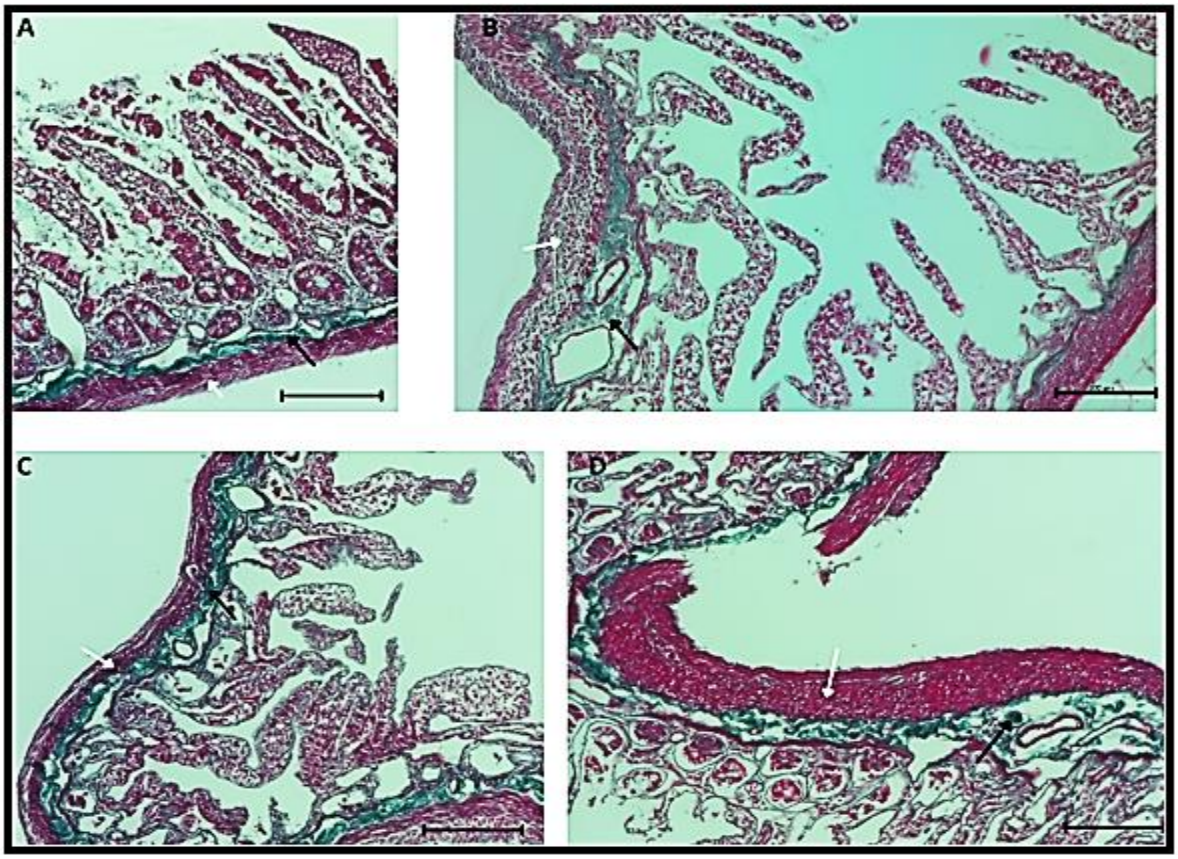

Figure 17. The photomicrographs show the mucosa of the jejunum stained with Masson trichrome illustrating the collagen fibres (green) in the submucosa (black arrow) and normal muscularis externa (white arrow) **A,** high density of collagen fibres in the submucosa layer (black arrow), increased thickness of the muscularis externa with increased collagen fibre content (white arrow) with transparent and permeable muscular wall **B**, reduction in area of collagen fibres in the submucosa (black arrow) and reduced thickness of the muscularis externa layer (white arrows) **C**, the area occupied by the collagen fibres has increased (black arrow) and thickness of the muscularis externa (black arrows)**D**. Scale bar=100µm.

4.4.2 Morphometrics associated with collagen fibre content in jejunum.

There was an increase in collagen fibre content in jejunum between control group and experimental animals, with mean collagen fibre content per unit area as follows: Group A (control) = 5726±201 per unit area, Group B (Alcohol) was 13327±134 per unit area, Group C (Combination Anti-Retroviral Therapy) was 7830±205 per unit area and Group D (Alcohol+ Combination Anti-Retroviral Therapy) was 8448±109 per unit area. There was statistically significant difference in collagen content between Group A and Group B; Group B and Group D ($p<0.05$) (Fig.18).

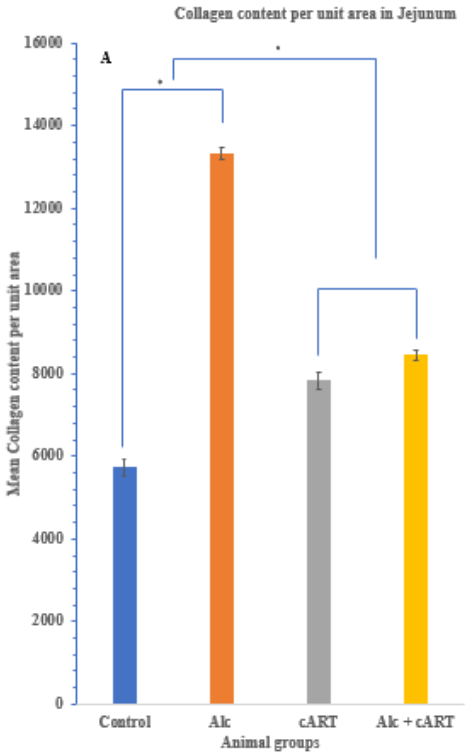

Figure 18. The effect of alcohol and/or cART therapy on the collagen fibre content in the jejunum of the Sprague-Dawley rats after 13-week treatment period. (A) Collagen fibre content per unit area. Bars indicate the mean±SD. Control group (Group A), Alcohol (Group B), Combination Anti-Retroviral Therapy (Group C) and Alcohol+ Combination Anti-Retroviral Therapy (Group D).

4.4.3 Collagen fibre content in walls of ileum segment of small intestines

Sections from ileum of Group A animals showed normal amount of collagen fibres (Fig. 19A.). The collagen fibre content has increased in submucosa of Group B (Fig. 19B). The intestinal section of Group C shows a marked decrease in collagen fibre content in submucosa (Fig.19C). The submucosa layer showed marked increase in area in Group D animals, but density of collagen fibres has decreased (Fig.19D).

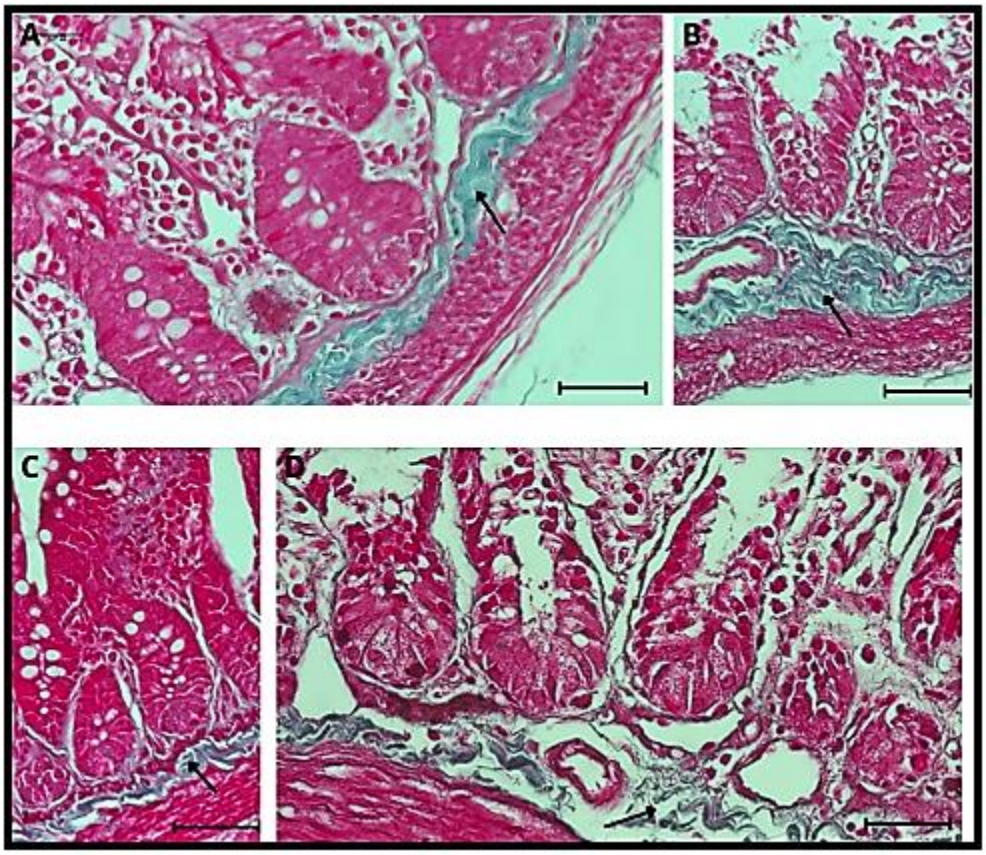

Figure 19. The photomicrograph shows the walls of the ileum stained with Masson trichrome illustrating the normal collagen fibre content (green) in the submucosa (black arrow) **A,** the collagen fibre content has increased (black arrow) **B**, reduction in the submucosa layer (area of collagen fibres) (black arrow) **C**, increase in the submucosa (reduced density of collagen fibres) (black arrow) **D**. Scale bar=20µm.

4.4.4 Morphometrics of collagen fibres in ileum

There was an increase in collagen fibre content in ileum between control group and experimental animals, with mean collagen fibre content per unit area as follows: Group A (control) = 3542±120 per unit area, Group B (Alcohol) was 11304±115 per unit area, Group C (Combination Anti-Retroviral Therapy) was 7637±250 per unit area and Group D (Alcohol + Combination Anti-Retroviral Therapy) was 11030±314 per unit area. There was statistically significant difference in the collagen content between Group A and Group B; Group A and Group C; Group A and Group D ($p<0.05$) (Fig.20).

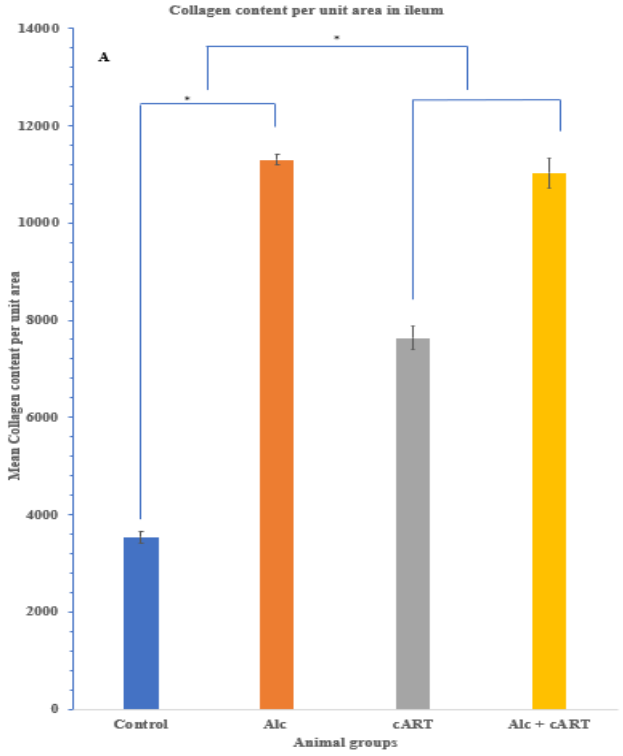

Figure 20. The effect of alcohol and/or cART therapy on the collagen fibre content in the ileum of the Sprague-Dawley rats after 13-week treatment period. (A) Collagen content per unit area. Bars indicate the mean±SD. Control group (Group A), Alcohol (Group B), Combination Anti-Retroviral Therapy (Group C) and Alcohol+ Combination Anti-Retroviral Therapy (Group D).

4.4.5 The histomorphological appearance of Paneth cells including their morphology and amounts of secretory granules, in the jejunum and ileum

4.4.5.1 The alpha defensin 5 immuno-appearance of Paneth cells, their morphology and amounts of secretory granules in the jejunum

The sections of specimens from control animals (Group A- saline treated animals) show unstimulated PCs with their nucleus irregularly shaped and occupying a third of the basal cytoplasm (Fig.21A). The mucosa of Group B (alcohol only treated animals) shows a low density of pyramidal shaped PCs with prominent and intensely stained granules (Fig.21B). Findings from animals in Group C (cART only treated animals) showed a high density of weakly stained Paneth cells with their broad bases resting on basement membrane and narrow apical ends with low amounts of stimulated secretory granules (Fig.21C). In Group D (cART+ alcohol treated animals), there is a high density of PCs that are irregularly shaped. The PCs are also distributed in proliferative zone of crypts (Fig.21D).

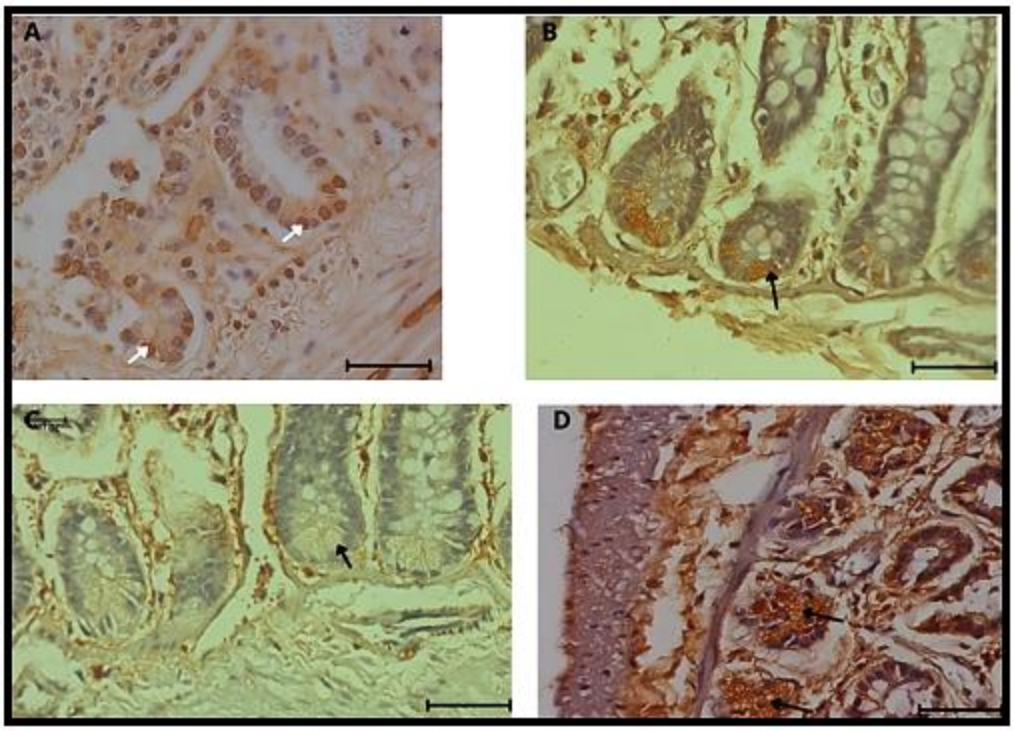

Figure 21. The photomicrograph shows the immunochemical detection of PCs in the mucosa of the jejunum using anti-alpha defensin 5. The unstimulated PC granules in the cytoplasm (white arrow) **A,** irregularly shaped PCs with high amount of α-defensin immune positive secretory granules (black arrow) **B**, a high density of weakly stained PCs (black arrow) **C**, a high density of irregularly shaped PCs with intensely stained stimulated secretory granules (black arrow) **D**. Scale bar=20µm.

4.4.5.2 Morphometrics of the appearance of Paneth cells immunoreactive to alpha defensin 5 in the crypts of the jejunum

There was an increase in PCs morphological score in jejunum between control group and experimental animals, with mean PC morphological score as follows: Group A (control) = 1±0.07, Group B (Alcohol) was 2±0.10, Group C (Combination Anti-Retroviral Therapy) was 1±0.14 and Group D (Alcohol+ Combination Anti-Retroviral Therapy) was 3±0.11. There was statistically significant difference in mean number mean PC morphological score between Group A and Group B ($p<0.05$), and Group B and Group C ($P<0.05$) (Fig.22A). The difference in the mean number of Paneth cells in animals in Group A and Group D was also statistically significant ($p<0.05$) and similarly, Group C and Group D ($p<0.05$) (Fig.22B). The mean anti-alpha defensin 5 antibody intensity increased with Group D = 3.5±0.05 Optical density as compared to 1±0.13 Optical density for Group A, with Group A and Group C ($p<0.05$) including Group B and Group D ($p<0.05$) being statistically significant ($p<0.05$) (Fig.23A).

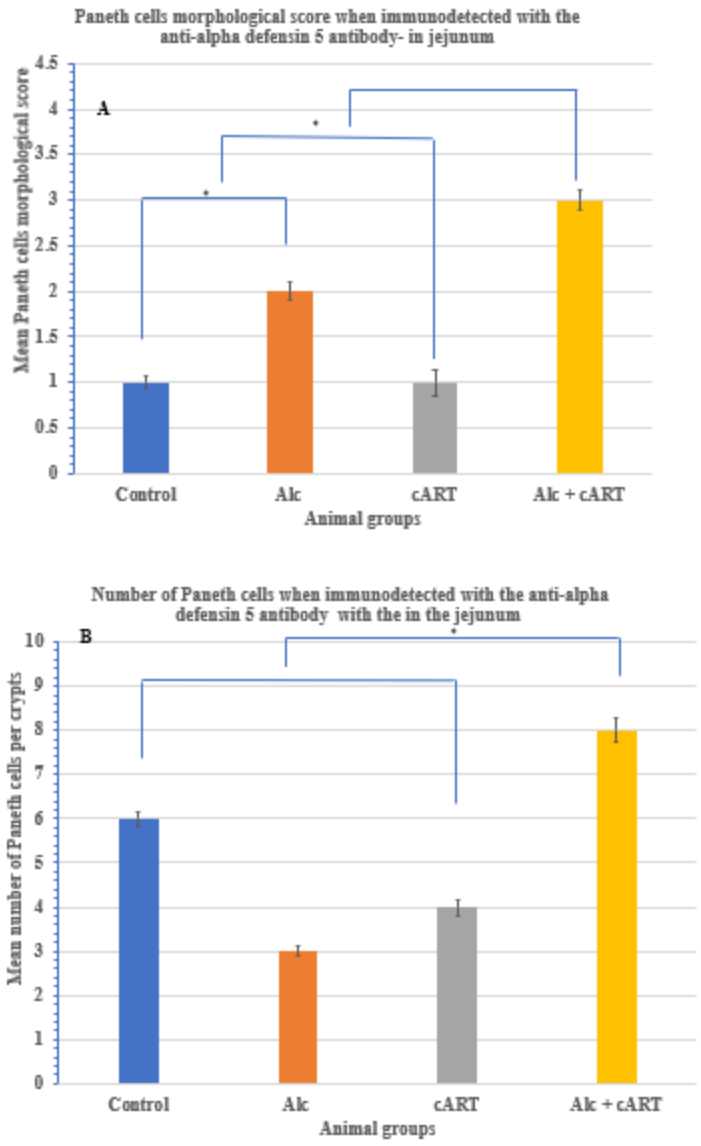

Figure 22. The effect of alcohol and/or cART therapy on the appearance of Paneth cells in the jejunum of the Sprague-Dawley rats after 13-week treatment period. (A) Paneth cells morphology score when immuno-detected with the Anti-alpha defensin 5 antibody (B)Number of Paneth cells when immuno-detected with the Anti-alpha defensin 5 antibody. Bars indicate the mean±SD. Control group (Group A), Alcohol (Group B), Combination Anti-Retroviral Therapy (Group C) and Alcohol+ Combination Anti-Retroviral Therapy (Group D).

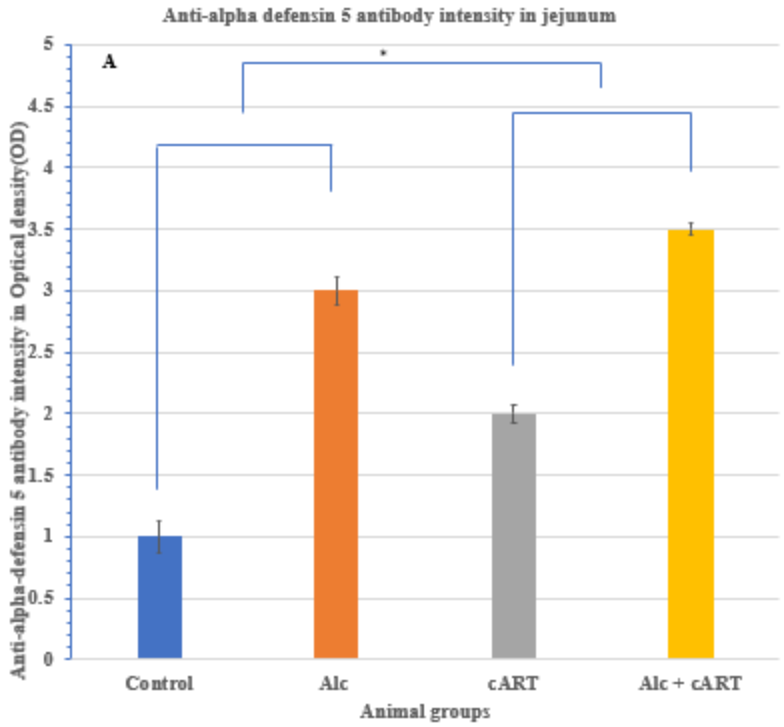

Figure 23. The effect of alcohol and/or cART therapy on the appearance of PCs in the jejunum of the Sprague-Dawley rats after 13-week treatment period. (A) Anti-alpha defensin 5 antibody intensity. Bars indicate the mean±SD. Control group (Group A), Alcohol (Group B), Combination Anti-Retroviral Therapy (Group C) and Alcohol+ Combination Anti-Retroviral Therapy (Group D).

4.4.5.3 The alpha defensin immune appearance of Paneth cells, their morphology and amounts of secretory granules in ileum.

Sections from ileum of Group A animals showed PCs with unstimulated granules (Fig. 24A.). PCs in Group B animals are pyramidal in shape, low density and have highly stimulated granules (Fig.24B). The PCs of Group C are unstimulated and low density (Fig. 24C). In Group D, the PCs are irregular in shape and in high density with large amounts of stimulated secretory granules. PCs are also visible in proliferation zone of crypts (Fig.24D).

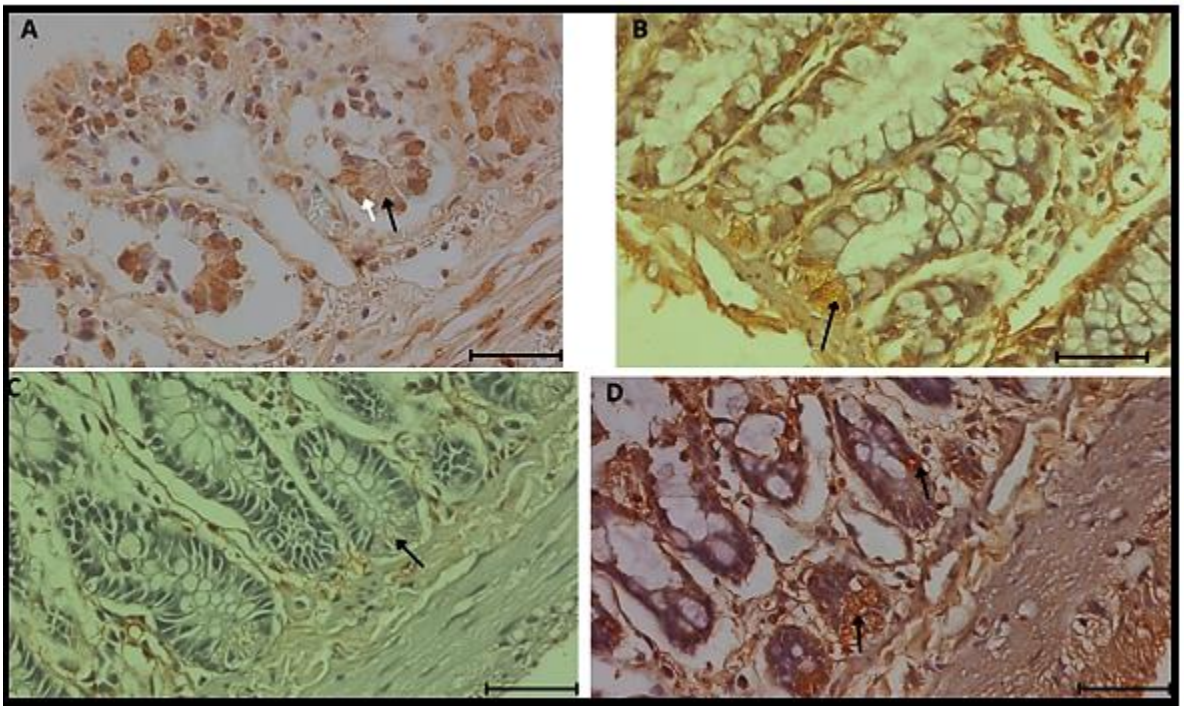

Figure 24. The photomicrographs show the immunochemical detection of PCs in the mucosa of the jejunum using anti-alpha defensin 5. Unstimulated PCs granules and their prominent nuclei (white arrow) **A,** a low density of pyramidal shaped PCs with high amount of α-defensins secretory granules (black arrow) **B**, unstimulated PCs (black arrow) **C**, medium density of irregularly shaped PCs with high stimulation of secretory granules. Some PCs are seen in proliferation zone (black arrow) **D**. Scale bar=20µm.

.

4.4.5.4 Morphometrics of appearance of Paneth cells immunoreactive to alpha defensin 5 in crypts of ileum

There was an increase in PCs morphological score in ileum between control group and experimental animals, with the mean PC morphological score as follows: Group A (control) = 1±0.13, Group B (Alcohol) was 2±0.21, Group C (Combination Anti-Retroviral Therapy) was 1±0.04 and Group D (Alcohol+ Combination Anti-Retroviral Therapy) was 3±0.12. There was statistically significant difference in mean number of PC morphological score between Group B and Group D ($p<0.05$), and Group C and Group D ($P<0.05$) (Fig.25A). The difference in mean number of PCs in animals in Group A and Group B was also statistically significant ($p<0.05$) and similarly, Group A and Group D ($p<0.05$) (Fig.25B). The mean anti-alpha defensin 5 antibody intensity increased in Group D, and it was 3.5±0.04 Optical density as compared to 1±0.07 Optical density for Group A, and the difference between Group A and Group B ($p<0.05$) and Group C and Group D ($p<0.05$) statistically significant ($p<0.05$) (Fig.26A).

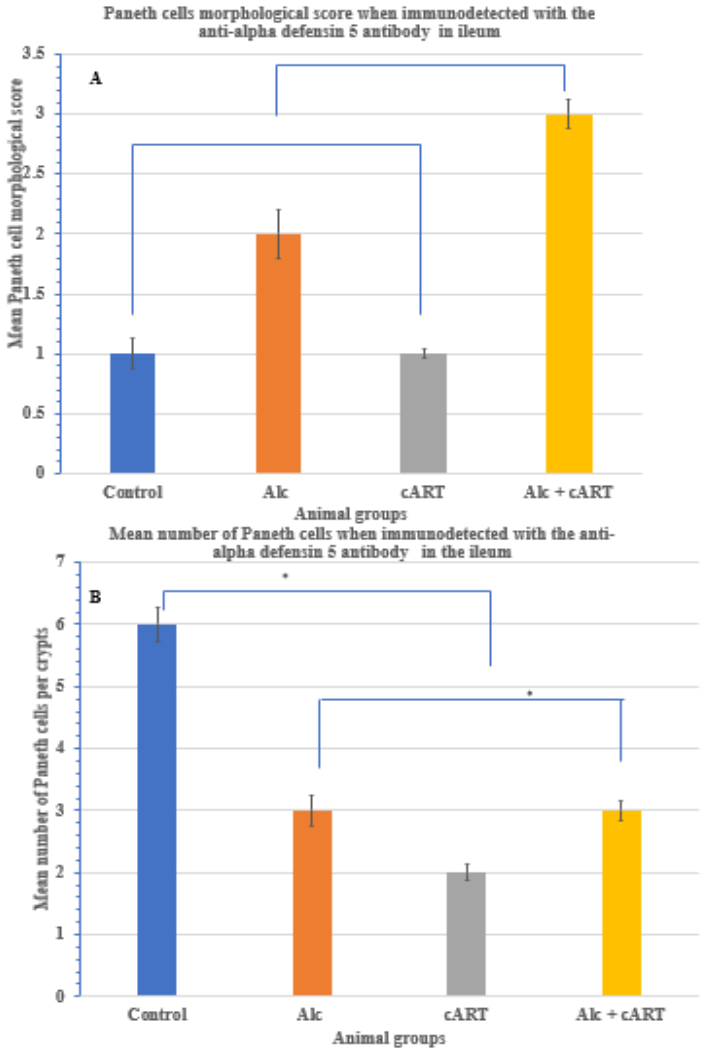

Figure 25. The effect of alcohol and/or cART therapy on the appearance of Paneth cells in the ileum of the Sprague-Dawley rats after 13-week treatment period. (A) Paneth cells morphology score when immunodetected with the Anti-alpha defensin 5 antibody (B) Number of Paneth cells when immunodetected with the Anti-alpha defensin 5 antibody. Bars indicate the mean±SD. Control group (Group A), Alcohol (Group B), Combination Anti-Retroviral Therapy (Group C) and Alcohol+ Combination Anti-Retroviral Therapy (Group D).

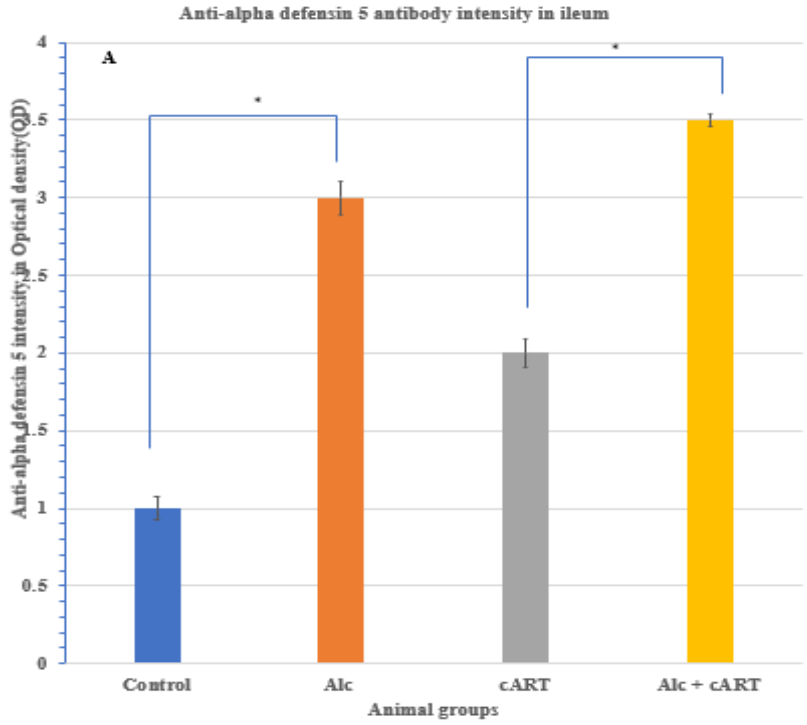

Figure 26. The effect of alcohol and/or cART therapy on the appearance of PCs in the ileum of the Sprague-Dawley rats after 13-week treatment period. (A) Anti-alpha defensin 5 antibody intensity. Bars indicate the mean±SD. Control group (Group A), Alcohol (Group B), Combination Anti-Retroviral Therapy (Group C) and Alcohol+ Combination Anti-Retroviral Therapy (Group D).

4.6 The histomorphological appearance of stem cells in the crypts of the jejunum and ileum

4.6.1 The histomorphological appearance of stem cells immunoreactive to anti-Musashi antibody in crypts of jejunum.

The sections of specimens from control animals (Group A- saline treated animals) showed high density of stem cells (SCs) in proliferation zone of crypts (Fig.27A). In the mucosa of Group B (alcohol only treated animals), there is low detection of SCs evidenced by weakly immunoreactivity (Fig.27B). Findings from animals in Group C (cART only treated animals) showed a high density of immuno-positive SCs that are intensely stained (Fig.27C). The SCs from Group D (cART+ alcohol treated animals) showed variation from normal shape and a low density of immunoreactive SCs (Fig.27D).

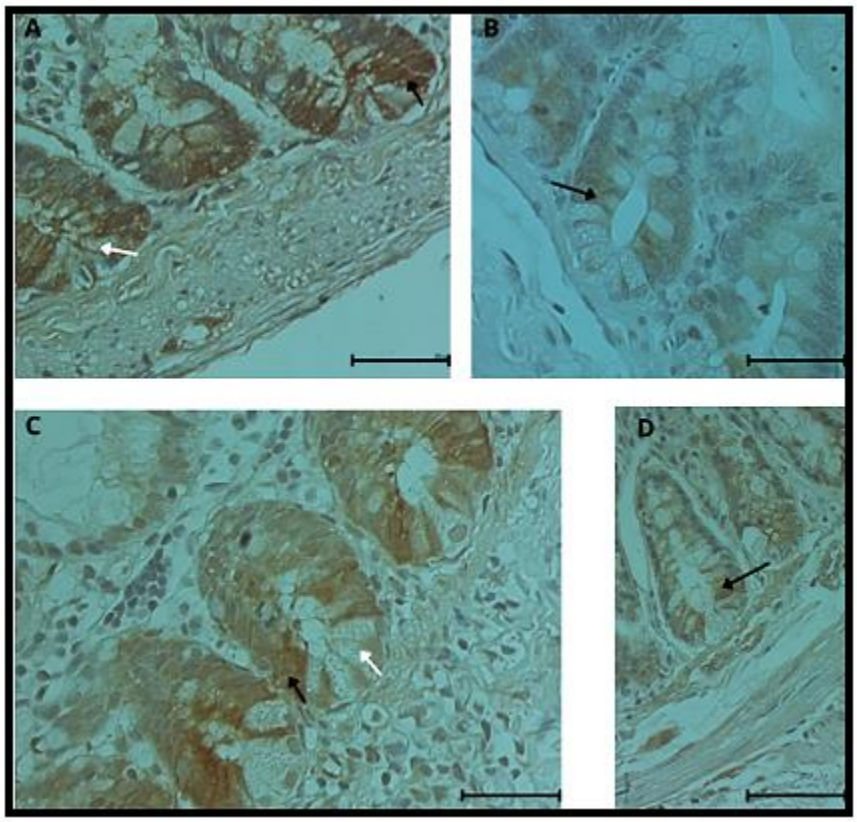

Figure 27. The photomicrograph shows the immunochemical detection of SCs in the mucosa of the jejunum using anti-Musashi-1antibody. The intestinal stem cells (black arrow) above PCs (white arrow) in the crypts **A,** rectangular shaped SCs with low intensity immunostaining (black

arrow) **B**, a high density of intensely labelled SCs (black arrow) intermingled with PCs (white arrow) C, variation in shape of SCs and weak staining in group D animals (black arrow) **D**. Scale bar=20µm

4.6.2 Morphometrics of appearance of stem cells immunoreactive to anti-Musashi antibody in crypts of jejunum

There was a change in appearance of SCs in jejunum between control group and experimental animals, with the mean stem cells morphological score as follows: Group A (control) = 1±0.09 (normal pyramidal Paneth cells present), Group B (Alcohol) =3±0.1 (non pyramidal Paneth cells identified), Group C (Combination Anti-Retroviral Therapy) =1±0.14 (normal pyramidal Paneth cells identified) and Group D (Alcohol+ Combination Anti-Retroviral Therapy) was 2±0.11 (normal pyramidal Paneth cells + non pyramidal Paneth cells identified). There was statistically significant difference in the mean stem cells morphological score between Group A and Group B ($p<0.05$), and Group C and Group D ($p<0.05$) (Fig.28A). There was a decrease in the intensity of the DAB stain in Group B and Group D when compared to the control Group A with the mean anti-Musashi-1antibody intensity in optical density (OD) as follows Group A (control) = 3.5±0.08 OD, Group B (Alcohol) =1±0.11, Group C (Combination Anti-Retroviral Therapy) = 3±0.05and Group D (Alcohol+ Combination Anti-Retroviral Therapy) was 1±0.06. There was statistically significant difference in mean stem cells morphological score between Group A and Group D ($p<0.05$), and Group B and Group C ($p<0.05$) (Fig.28B).

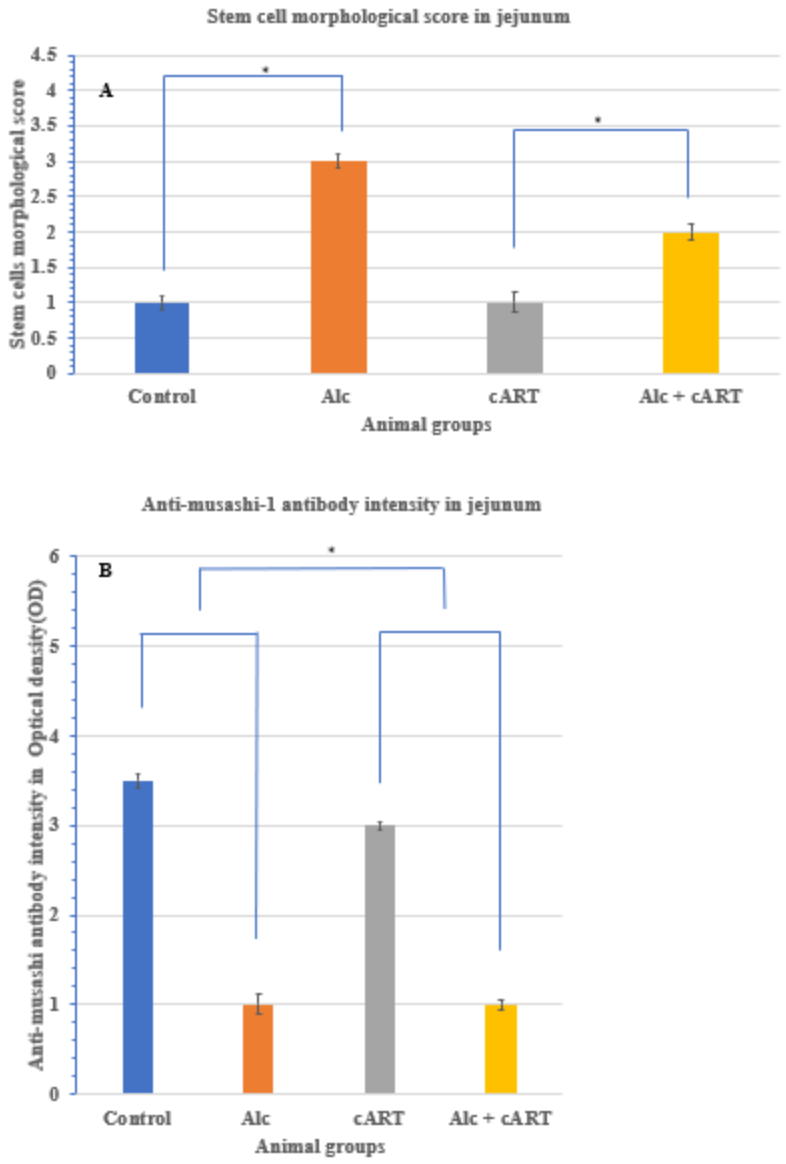

Figure 28. The effect of alcohol and/or cART therapy on the appearance of stem cells in the jejunum of the Sprague-Dawley rats after 13-week treatment period. (A) stem cells morphology score (B) Anti-Musashi antibody intensity. Bars indicate the mean±SD. Control group (Group A), Alcohol (Group B), Combination Anti-Retroviral Therapy (Group C) and Alcohol+ Combination Anti-Retroviral Therapy (Group D).

4.6.3 The histomorphological appearance of stem cells immunoreactive to anti-Musashi antibody in the crypts of the ileum.

Sections from the ileum of Group A animals showed SCs in proliferation zone above Paneth cells (Fig.29A). SCs in Group B animals are weakly stained, in medium density and located in proliferation zone of crypt (Fig.29B). The intestinal SCs of Group C are in high density and located in both proliferation and basal zone (Fig.29C). The stem cells are in medium density with low intensity staining located in proliferation zone of crypts in Group D (Fig.29D).

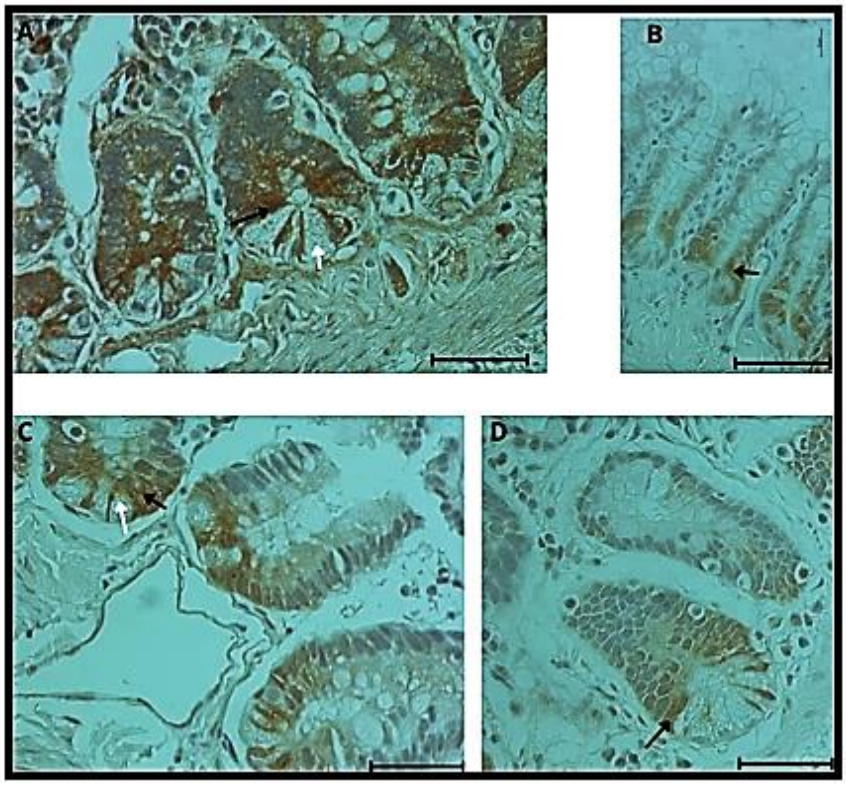

Figure 29. The photomicrograph shows the immunochemical detection of SCs in the mucosa of the ileum using anti-Musashi-1antibody. The intestinal stem cells (black arrow) above PCs (white arrow) **A,** a medium density of SCs, moderately stained (black arrow) **B**, a high density of intensely stained SCs (black arrow) located in the proliferation zone and the base of crypt together with PCs (white arrow) C, a low density of weakly stained stem cells (black arrows) above the PCs (black arrow) **D**. Scale bar=20µm.

4.6.4 Morphometrics of appearance of stem cells immunoreactive to Anti-Musashi antibody in crypts of ileum

There was a change in appearance of SCs in ileum between control group and experimental animals, with mean stem cells morphological score as follows: Group A (control) was 1±0.11 (normal pyramidal Paneth cells present), Group B (Alcohol) was 3±0.08 (non pyramidal Paneth cells identified), Group C (Combination Anti-Retroviral Therapy) was 1±0.13 (normal pyramidal Paneth cells identified) and Group D (Alcohol+ Combination Anti-Retroviral Therapy) was 2±0.12 (normal pyramidal Paneth cells + non pyramidal Paneth cells identified). There was statistically significant difference in mean stem cells morphological score between Group A and Group D and Group B and Group C ($p<0.05$) (Fig.30A).

There was a decrease in intensity of DAB stain in Group B and Group D when compared to control Group A with mean anti-Musashi-1antibody intensity in optical density (OD) as follows Group A (control) was 3.5±0.07 OD, Group B (Alcohol) was 2±0.02, Group C (Combination Anti-Retroviral Therapy) was 3.5±0.04 and Group D (Alcohol+ Combination Anti-Retroviral Therapy) was 1.5±0.09. There was statistically significant difference in mean anti-Musashi-1antibody intensity in optical density (OD) between Group A and Group B; Group A and Group B and Group A and Group D ($p<0.05$) (Fig.30B).

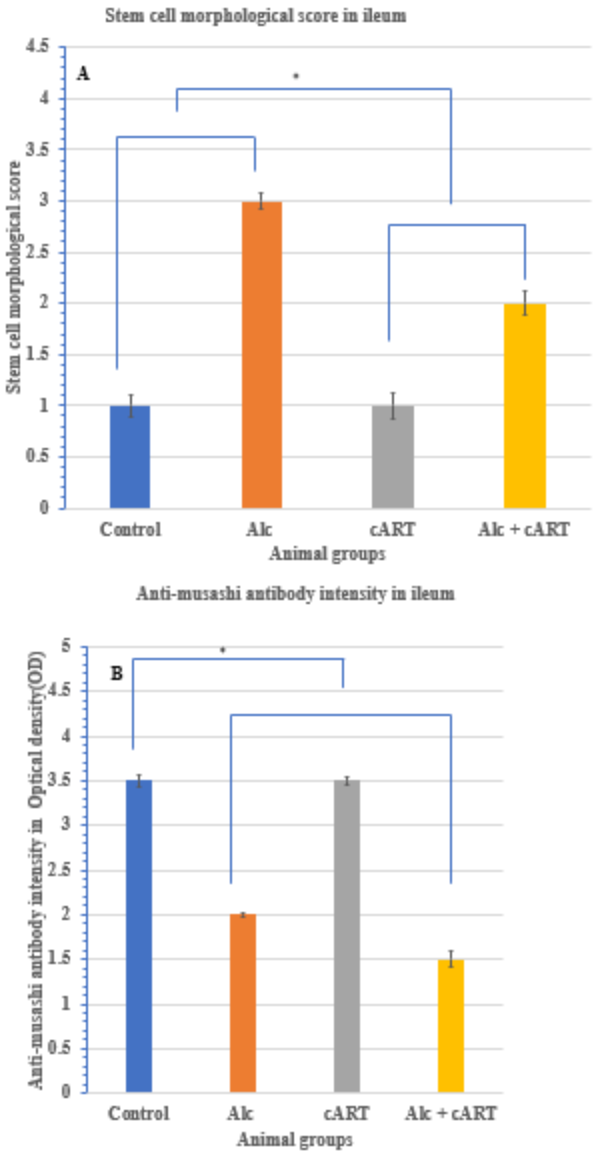

Figure 30. The effect of alcohol and/or cART therapy on the appearance of stem cells in the ileum of the Sprague-Dawley rats after 13-week treatment period. (A) stem cells morphology score(B)Anti-Musashi antibody intensity. Bars indicate the mean±SD. Control group (Group A), Alcohol (Group B), cART (Group C) and Alcohol+ cART(Group D).

Chapter 5: Discussion

5.1 Introduction

The study evaluated the histomorphologic appearances of Paneth cells and crypt-villous morphology in small intestine of rats exposed to alcohol and/or combination anti-retroviral therapy (cART). The study achieved this by evaluating the morphometric changes of the crypts and villi dimensions in the jejunum and ileum, determining the location of Paneth cells along the axis of the intestinal crypts of the jejunum and ileum, examining the histomorphological appearance of Paneth cells including their morphology and amounts of secretory granules, in the jejunum and ileum and by examining the histomorphological appearance of stem cells in the crypts of the jejunum and ileum. Morphometry and morphological analysis showed significant ($p < 0.05$) reduction in villous height, villous width, crypt's depth, intestinal stem cells, increased villous stripping, increased crypt's width, increased muscular wall thickness, increased number of Paneth cells and staining intensity of Paneth cell granules in alcohol + cART treated group. Paneth cells were noted in the proliferation zone of small intestines of animals that had combined treatment (alcohol +cART).

5.2 Morphometric changes of crypts and villi dimensions in the jejunum and ileum

In the present study, we observed alcohol and combination anti-retroviral therapy (Atripla) - induced alteration of small intestinal epithelium. This study is first study of its kind to present the morphometric analysis of number of villi, number of crypts, wall thickness, villous height, and width; crypts depth and width in small intestine following treatment with alcohol and/or ARVs.

Alcohol was utilized since several alterations of small-intestinal morphology and function have been documented after its ingestion (Bishehsari et al., 2017, Persson, 1991). Combination anti-retroviral drug (Atripla) was utilized since it is a fixed-dose combination ARV tablet. The drug contains efavirenz, emtricitabine, and tenofovir. Efavirenz is an inhibitor of CYP 450 3A4, an enzyme that oxidizes alcohol before it is eliminated from the body. When efavirenz is administered concomitantly, effects of alcohol are increased (Imhof et al., 2001).

The study observed a similar trend in jejunum and ileum in all parameters which were measured, whereby in both segments of intestines there was an increase in number of villi following treatment with alcohol and/or combination anti-retroviral drug (Atripla). The main purpose of the villi is to increase surface area in intestine for absorption of nutrients (Mah 2014). The increase in number of villi increases surface area for digestion (Mah et al., 2014). The villi are joined to crypts through crypt-villous junction. In a healthy mucosa two villi are linked together by one crypt (Gulbinowicz, 2004). If there is an increase in the number of villi, the crypts will also increase since they are connected, and the results of the present study confirmed such increases in both the villi and crypts in jejunum and ileum. Studies have shown that small intestinal epithelium is highly responsive to changes in nutrient intake or exposure to luminal nutrient (Zoubi et al., 1994, Bindseil and Christensen, 1984, Gaudino et al., 2021, Park et al., 2021).

A study by Gulbinowicz (2004) found that in rodents, fasting or total parenteral nutrition leads to rapid reduction in small intestinal epithelial mass, associated with reduced proliferation in crypts and increased apoptosis in crypts and villi. However, this study found that villi and crypts were increased but, in some places, crypts were properly discerneable, suggesting atrophic changes due to the treatment. Since the treatment started increasing appetite of rats, they started consuming more of it, it then led to changes such as reduction in villous height and width causing villous atrophy, blunting, and stripping of all essential layers and microvilli.

Villous atrophy is considered the gold standard for diagnosing celiac disease (CD) and its complications (O'Farrelly, 2000).Villous atrophy has been also been reported in small intestines as a histological change following HIV infection (Bjarnason et al., 1996, Zeitz et al., 1998, Johanson, 1996). Villi may be blunted and shortened or appear atrophic when lamina propria is infiltrated by macrophages, such as in Whipple's disease or in Mycobacterium avium intracellular infections, or by a dense infiltrate of plasma cells and centrocyte-like lymphocytes or small, pleomorphic lymphocytes (Strauch and Scholmerich, 1996). There is very little information reported in literature regarding villus stripping (Gaudino et al., 2021, Park et al., 2021). In conditions that involve villus stripping, lacteal vessels in core of villus are usually preserved (Holle 1991), even after villi were eroded of all essential layers.

The current study found that treatment with alcohol and/or Combination Anti-Retroviral Therapy (Atripla) caused a decrease in depth of crypts and an increase in crypts width, which caused crypts to become flatter and more indiscernible from lining epithelium. Disruption of intestinal crypts is abnormal and is associated with celiac disease (Pluske et al., 1996). The functional integrity of small intestines relies on adult stem cells which are found at the base of intestinal crypts that proliferate and differentiate into multiple functionally distinct cell types. The progenies of intestinal stem cells migrate upward to the villus tips and are eventually shed into the lumen of gut. Without crypts housing these stem cells this tight coordination fails, resulting in poor regeneration of intestinal epithelium and intestinal diseases (Cheng et al., 1986).

The combination of alcohol and cART caused the muscularis externa layer of small intestine to become thicker for which several studies have shown that a wide variety of intestinal diseases lead to thickening of wall of small intestine which may be visualized on computed tomography (Persson, 1991). Common causes of bowel wall thickening include edema, hemorrhage, infection, graft-versus-host disease, and inflammatory bowel disease rare causes of thickening of wall of small intestine also include immunodeficiencies, lymphoma, hemangioma, pseudotumor, and Langerhans cell histiocytosis (d'Almeida et al., 2008). An increase in thickness of muscular wall may cause the wall to be less tight or compact, leading to an increase in permeability causing it to be inflamed. Gastrointestinal inflammation results from an inflammatory response caused by immune system against alcohol and its metabolites (Bishehsari et al., 2017)

A study conducted by Park and colleagues in 2021 showed that excessive alcohol consumption damages mucosal barrier of the GIT, which may lead to inflammation and a wide variety of cancers, especially in small intestine (Park et a., 2021). Increased intestinal permeability, mucosal damage, and inhibition of water absorption are observed following excessive consumption of alcohol (Park et al., 2021). Another study recently found a significant increase in mucosal thickness following total celiac and superior mesenteric ganglionectomy (Holle, 1991).

5.3 The location of Paneth cells along the axis of intestinal crypts of jejunum and ileum.

Several studies have reported a change in density of Paneth cells (PC) in intestinal crypts, and their location along crypt-villous axis as well as in their cytoplasmic granule under certain pathological conditions (Lueschow and McElroy, 2020, Gassler, 2017, Garabedian et al., 1997, Kelly et al.,

2004, Holly et al., 2017). this current study, different techniques were used to evaluate density and location of PCs and concentration of their granules in the small intestine of rats exposed to alcohol and/or cART (Atripla) was used. Exposure to alcohol and cART (Atripla) caused some of PCs to fail to migrate from proliferation zone to base of crypt Paneth cells are termed 'metaplastic' when seen in areas in which they are not normally found Paneth cell metaplasia (PCM) has been described in idiopathic inflammatory bowel disease (IBD), both ulcerative colitis (UC) and Crohn's disease (CD). In adults, it is thought to be a sign of a long colitis history it correlates with disease duration, and it has been attributed to the effects of repair and regeneration (Simmonds et al.,2014, Tanaka et al.,1974, Symonds,1974)

The proliferative zone of epithelium of small intestine contains undifferentiated and rapidly cycling stem cells that populate crypts of Lieberkühn. Unlike the rest of differentiated cells which migrate upwards in crypts, PCs migrate towards crypt base (Ganz, 2000) with more mature PCs occupying the base of crypts (Dipankar Ghosh, 2000). This then means that combination of alcohol and cART (Atripla) was causing rapid recycling of naïve immature PCs hence they were seen in proliferation zone. Exposure to alcohol and cART may have triggered Paneth cells' defense mechanism. The current study also found that there was a lower number of PCs and a reduction in concentration of their granules in proliferation zone (zone 2), this was because large amounts of granules are produced by older and more mature cells. The PCs in zone 2 are immature and naïve hence lower density of PCs containing fewer granules (Garabedian et al., 1997).

Combination Anti-Retroviral Therapy (cART) with alcohol caused a reduction in density of PCs, but increase in cytoplasmic granules seen by intensity of the stain, a study conducted in 2010 found the opposite from current study ,where Rhesus macaques with simian AIDS (SAIDS) due to chronic SIV infection had increased density of PCs per crypt but Paneth cells showed reduced numbers of cytoplasmic granules (Estes et al., 2010) . The anti-microbial peptides which are secreted by PCs have strong anti-microbial activities against a range of bacteria, fungi, parasites, and viruses (Holly et al., 2017). They regulate the composition of gut microbiota. If there is a reduction in the granules and they are less intense, the GIT becomes susceptible to colonization by harmful pathogens (Dipankar Ghosh, 2000).

5.4. Collagen fibre content in the wall of jejunum and ileum of small intestines

The current study found that the interaction between alcohol and cART (Atripla) causes a change in the density of collagen fibres in the submucosal layer this could have been caused by the simultaneous conversion of these two drugs since the enzyme which are needed to breakdown alcohol in the liver into acetaldehyde were also breaking down the cART (Cohen et al.,2011;McCance-Katz, 2016).

The architecture and function of an organ are determined to a larger extent by amount, distribution, organization, and types of collagen fibres present in the extracellular matrix (Zeng et al., 2003). In normal tissue submucosal layer consists almost entirely of collagen which is called skeleton of small intestine (Yu et al., 2004). A derangement in one or more of these aspects of collagenous matrix can lead to a significant structural and functional disturbance in an organ (Zeng et al., 2003). An increase in collagen content with thickening of the muscular wall may lead to narrowing of small intestine. Very little is known about the stricture formation of collagen in human bowel either in health or disease (Yu et al., 2004). Stricture formation is a common phenomenon in Crohn's disease and often occurs early in the course of the disease (Zeng et al., 2003). The narrowing of the lumen of gut causes partial to complete obstruction that in turn contributes to chronic anorexia, malnutrition, weight loss, and failure of linear growth and sexual maturation in children (Yu et al., 2004). Surgical resection is frequently required but the process often recurs and cycle of inflammation, stricturing, and surgery is repeated (Zeng et al., 2003).

Strictures can also complicate peptic, ischemic, and other inflammatory processes in gastrointestinal tract. Despite the high morbidity associated with strictures in Crohn's and other diseases, mechanism through which chronic inflammation leads to stricturing of bowel is unknown and is currently vaguely conceptualized as a progressive "thickening" of bowel wall (Gallo et al., 2021). Collagenous colitis (CC) is one type of inflammatory bowel disease. The inflammation on the wall of the gut causes extra collagen to build up on the wall of the small intestine leading to episodes of watery diarrhea and belly pain which are some of reported side effects of Combination Anti-Retroviral Therapy (Atripla) (Windon et al., 2020). Having Coeliac disease increases the risk of having CC, Coeliac disease has been found to be associated with combination of alcohol and Atripla in current study meaning one is at higher risk of having CC and IBD when taking alcohol and ARV's concurrently.

5.5 The histomorphological appearance of Paneth cell including their morphology and amounts of secretory granules, in the jejunum and ileum.

Paneth cells originate from stem cells (SC) at the SC region that is near the bottom of intestinal crypt. Unlike the other epithelial cell types, Paneth cells migrate downward from SC region and settle just adjacent to it hence intestinal SCs are intermingled with PCs. Paneth cells secretions are involved in nourishment of stem cells and for keeping intestinal stem cell zone sterile. In control group study found a well-preserved architecture of PCs with prominent nuclei but with low stimulation of PCs and their secretory granules which was evidenced by low intensity staining. Low stimulation of Paneth cell granules observed is since PCs are stimulated by a microbial insult and respond by releasing antimicrobial substances such as α-defensins peptide hence, in the absence of a stimuli Paneth cells and their secretory granules will not be stimulated (Tobi et al., 2021). The main roles of PCs involve package and export of a variety of antimicrobial proteins and peptides in order to protect intestinal mucosa against a wide range of bacteria, fungi, parasites, and viruses (Holly et al., 2017). They determine and maintain composition of the gut microbiota.

The granules of PCs are rich in α-defensins, which contribute to enteric innate immunity to infection and determine composition of small intestinal microbiota (Iyer and Vaishnava, 2016). This study used Alpha-defensin-5 antibody for immunochemical detection of Paneth cells because enteric α-defensins are most abundant of the secreted products and to quantify PC numbers, expression of α-defensin antimicrobial peptide and to observe any morphological changes that may be caused by the treatment.

Exposure to Alcohol caused a change in morphology of PCs, reduction in number of PCs and high production of α-defensin-5 antimicrobial peptide, PCs are pyramidal formed cells with prominent eosinophilic granules (Ehrmann et al., 1990). Any alteration to morphology of PCs results in both structural and immunological abnormalities (Batman et al., 2007). Reduction in total number of PCs has been reported in patients who have coeliac disease, other diseases including malnutrition, parasitic infection, and HIV/AIDS (Tobi et al., 2021). An up-regulation of HD5 in colorectal mucosa has been observed in patients with HIV-1, possibly in response to intestinal inflammation (Holly et al., 2017).

Defensins and other antimicrobial peptides which are secreted by PCs regulate composition of intestinal microbiota and prevent colonization of the intestinal crypt environment by harmful

pathogens (Dipankar Ghosh, 2000). Suppressed PCs secrete fewer antibacterial compounds, which can allow intestinal bacteria overgrowth leading to over production of by-products such as endotoxins and their subsequent leakage through intestinal barrier, even though the current study showed a high production of these antimicrobial peptides in alcohol exposed animal group a reduction in the number of PCs was also observed (Imhof et al., 2001).

PCs secrete α-defensins and adenosine monophosphates in response to cholinergic stimulation, Alcohol may interfere with cholinergic stimulation thereby reducing Paneth cell activity and this may lead to bacterial overgrowth and resident microbiota becoming proinflammatory leading to disease(Zhou et al., 2020).

The current study found that combination of alcohol and cART (Atripla) mimicked microbial signals as evidenced by increase in intensity of secretory granules. During pathology, exposure of microbial signals cause PCs to release their microbicidal granule contents into gut lumen (Ayabe et al., 2000). cART augmented the effects of alcohol when these drugs were administered concomitantly because it contains ritonavir and ritonavir an inhibitor of CYP 450 3A4 an enzyme responsible for detoxifying alcohol, hence, damage caused by alcohol is amplified in this situation (Imhof et al., 2001).

The interaction between alcohol and cART also caused an increase in number of non-pyramidal shaped Paneth cells / dysfunctional Paneth cells exposing gut to ulcerative colitis, tuberculous typhlitis and tumors(Iyer and Vaishnava, 2016, Lewin and Rouzioux, 2011, Sommers, 1966, Voshavar, 2019). Studies show that alcohol can directly modulate both innate and adaptive immunity, further contributing to gut and gut-derived inflammation(Bishehsari et al., 2017, Bagasra et al., 1993, Samet et al., 2007). A study in mice found that alcohol inhibits intestine's immune response for clearing harmful bacteria (Llopis et al., 2016). Another separate study found that alcohol suppresses intestinal mucosal immune cell activity (Imhof et al., 2001).

PCs have long been recognized for their remarkable morphological attributes(Al-Saffar, 2016). Now, the understanding of their biology implicates PC α-defensins in immunity to enteric infection, in maintenance of the small bowel crypt stem cell population and in determining composition of the small intestinal microbiome (Salzman et al., 2010). In view of the diversity of biologically active peptide and protein constituents in PC secretory granules, influence of Paneth cells on intestinal health and homeostasis cannot be over emphasized (Lin et al., 2022). With

complete discovery of a spectrum of genes whose variant products induce or predispose to inflammation of intestinal mucosa, understanding of molecular basis of PCs involvement in disease along with new therapeutic targets for intervention will be improved (Shankman et al., 2021).

5.6 The histomorphological appearance of stem cells in the crypts of the jejunum and ileum.

Paneth cells secretions are involved in nourishment of stem cells (SC) and also keeping intestinal stem cell zone sterile (Lencer, 1998). Excessive alcohol can induce intestinal damage leading to intestinal bowel diseases (Shankman et al., 2021). Thus, control of small intestinal epithelial cell regeneration is thought to be important for homeostasis in response to epithelium damage (Park et al., 2021). However, reports on how epithelial cells respond to small intestinal damage caused by a combination of alcohol and cART (Atripla) is scarce.

The current study found that in the control and cART exposed groups there was high immunodetection of SCs by anti-Musashi antibody as shown by intensity of staining, during regenerative episodes newly formed intestinal cell are sustained (McCauley et al., 2020), hence we saw a great preservation of SCs in the control group and cART treated group. In addition, results suggest that cART did not have any negative effects on SCs since appearance and concentration of SCs were sustained.

Combination of alcohol and cART (Atripla) cause low detection of SCs and change of normal morphology and several metabolic syndromes cause alteration in stem cell niche, including presence or absence of specific metabolities (Al-Saffar, 2016).The most common underlying pathologies include obesity ,diabetes, hypercholesterolemia and endocrine disorders(Clarke, 2005)

Intestinal SCs are responsible for extremely rapid renewal of entire epithelial lining, they are multipotent and generate all cell types of intestinal lineage, comprising enterocytes, goblet cells, endocrine cells, and PCs (Kwon et al., 2022). All these cells are distributed across the surface of intestine, according to a precise topography (Yokoi et al., 2019). The proliferation compartment is located in crypt, while differentiation compartment is situated in villus. The more cells are specialized, the more they migrate from bottom of crypt to lumen of intestine (Pinto and Clevers, 2005). This means exposure to alcohol was causing rapid differentiation of SCs into these specialized cells, and or death hence the reason for low density of SCs. Any change in morphology

of SC will affect their physiological function, including absorption and endocrine/exocrine functions and resulting in cancer since cancer is a stem cell disease (Khaloian et al., 2020).

Intestinal stem cells are responsible for extremely rapid renewal of entire epithelial lining(Park et al., 2021). The maintenance of critical absorptive function of gut relies on appropriate control of the stem cell pool by local micro-environment or niche cell (Shankman et al., 2021). So, any imbalance caused by any external factor could mean loss of entire epithelial lining. Any structural change in small intestine, ISC and PCs may adversely affect regulation gut innate immunity incessantly and loss of gut immunity means adverse outcomes of infections and possibly death.

Chapter 6: Conclusion

Concomitant use of alcohol and cART led to thickening of small intestinal wall, shortening and/or stripping villi, reduction of crypt depth, appearance of Paneth cells in proliferation zone and a decrease in intestinal stem cells. The structural changes in small intestine and Paneth cells may adversely affect the regulation of gut innate immunity. These findings are clinically invaluable in management of HIV patients considering the critical significance of innate immunity amongst HIV patients.

Chapter 7: Recommendations

1. Double detection of stem cells and Paneth when exposed to alcohol to see the effects on both cells.
2. Double detection or labelling of stem cells and Paneth when exposed to both alcohol and cART
3. Further investigation into the complex relationship between α-defensins and HIV pathogenesis in HIV patients' specimens.

REFERENCES

AL-SAFFAR, F. J. A. A.-H., A.G., 2016. Al-Saffar, F.J. and Al-Haik, A.G., 2016. Histomorphological relationship of paneth cells with stem cells in the small intestine of indigenous rabbit at different postnatal ages.

BAGASRA, O., KAJDACSY-BALLA, A., LISCHNER, H. W. & POMERANTZ, R. J. 1993. Alcohol intake increases human immunodeficiency virus type 1 replication in human peripheral blood mononuclear cells. *J Infect Dis,* 167**,** 789-97.

BATMAN, P. A., KOTLER, D. P., KAPEMBWA, M. S., BOOTH, D., POTTEN, C. S., ORENSTEIN, J. M., SCALLY, A. J. & GRIFFIN, G. E. 2007. HIV enteropathy: crypt stem and transit cell hyperproliferation induces villous atrophy in HIV/Microsporidia-infected jejunal mucosa. *AIDS,* 21**,** 433-9.

BERKOWITZ, L., PARDO-ROA, C., RAMIREZ, G., VALLEJOS, O. P., SEBASTIAN, V. P., RIEDEL, C. A., ALVAREZ-LOBOS, M. & BUENO, S. M. 2019. The absence of interleukin 10 affects the morphology, differentiation, granule content and the production of cryptidin-4 in Paneth cells in mice. *PLoS One,* 14**,** e0221618.

BEVINS, C. L. & SALZMAN, N. H. 2011. Paneth cells, antimicrobial peptides and maintenance of intestinal homeostasis. *Nat Rev Microbiol,* 9**,** 356-68.

BINDSEIL, E. & CHRISTENSEN, N. O. 1984. Thymus-independent crypt hyperplasia and villous atrophy in the small intestine of mice infected with the trematode Echinostoma revolutum. *Parasitology,* 88 (Pt 3)**,** 431-8.

BISHEHSARI, F., MAGNO, E., SWANSON, G., DESAI, V., VOIGT, R. M., FORSYTH, C. B. & KESHAVARZIAN, A. 2017. Alcohol and Gut-Derived Inflammation. *Alcohol Res,* 38**,** 163-171.

BJARNASON, I., SHARPSTONE, D. R., FRANCIS, N., MARKER, A., TAYLOR, C., BARRETT, M., MACPHERSON, A., BALDWIN, C., MENZIES, I. S., CRANE, R. C., SMITH, T., POZNIAK, A. & GAZZARD, B. G. 1996. Intestinal inflammation, ileal structure and function in HIV. *AIDS,* 10**,** 1385-91.

BOULLE, A., BOCK, P., OSLER, M., COHEN, K., CHANNING, L., HILDERBRAND, K., MOTHIBI, E., ZWEIGENTHAL, V., SLINGERS, N., CLOETE, K. & ABDULLAH, F. 2008. Antiretroviral therapy and early mortality in South Africa. *Bull World Health Organ,* 86**,** 678-87.

BRENCHLEY, J. M. & DOUEK, D. C. 2008. HIV infection and the gastrointestinal immune system. *Mucosal Immunol,* 1**,** 23-30.

CELLO, J. P. & DAY, L. W. 2009. Idiopathic AIDS enteropathy and treatment of gastrointestinal opportunistic pathogens. *Gastroenterology,* 136**,** 1952-65.

CHENG, H., BJERKNES, M., AMAR, J. & GARDINER, G. 1986. Crypt production in normal and diseased human colonic epithelium. *Anat Rec,* 216**,** 44-8.

CIHLAR, T. & FORDYCE, M. 2016. Current status and prospects of HIV treatment. *Curr Opin Virol,* 18**,** 50-6.

CIHLAR, T. & RAY, A. S. 2010. Nucleoside and nucleotide HIV reverse transcriptase inhibitors: 25 years after zidovudine. *Antiviral Res,* 85**,** 39-58.

CLARKE, R. B. 2005. Isolation and characterization of human mammary stem cells. *Cell Prolif,* 38**,** 375-86.
CLEVERS, H. C. & BEVINS, C. L. 2013. Paneth cells: maestros of the small intestinal crypts. *Annu Rev Physiol,* 75**,** 289-311.
COHEN, C., ELION, R., RUANE, P., SHAMBLAW, D., DEJESUS, E., RASHBAUM, B., CHUCK, S. L., YALE, K., LIU, H. C., WARREN, D. R., RAMANATHAN, S. & KEARNEY, B. P. 2011. Randomized, phase 2 evaluation of two single-tablet regimens elvitegravir/cobicistat/emtricitabine/tenofovir disoproxil fumarate versus efavirenz/emtricitabine/tenofovir disoproxil fumarate for the initial treatment of HIV infection. *AIDS,* 25**,** F7-12.
D'AGOSTINO, C., LICHTNER, M., MASTROIANNI, C. M., CECCARELLI, G., IANNETTA, M., ANTONUCCI, S., VULLO, V. & MASSETTI, A. P. 2009. In vivo release of alpha-defensins in plasma, neutrophils and CD8 T-lymphocytes of patients with HIV infection. *Curr HIV Res,* 7**,** 650-5.
D'ALMEIDA, M., JOSE, J., ONETO, J. & RESTREPO, R. 2008. Bowel wall thickening in children: CT findings. *Radiographics,* 28**,** 727-46.
DENG, G., LEI, Q., GAO, X., ZHANG, Y., ZHENG, H., BI, J. & WANG, X. 2021. Glucagon-Like Peptide-2 Modulates Enteric Paneth Cells Immune Response and Alleviates Gut Inflammation During Intravenous Fluid Infusion in Mice With a Central Catheter. *Front Nutr,* 8**,** 688715.
DIPANKAR GHOSH, E. P., BO SHEN, SARAH K. LEE, DENNIS WILK, JUDITH DRAZBA, SATYA P. YADAV, JOHN W. CRABB, TOMAS GANZ & CHARLES L. BEVINS 2000. Paneth cell trypsin is the processing enzyme for human defensin-5. *1(2),* , 1(2), **,** 113-118.
EGOROV, V. I., SCHASTLIVTSEV, I. V., PRUT, E. V., BARANOV, A. O. & TURUSOV, R. A. 2002. Mechanical properties of the human gastrointestinal tract. *J Biomech,* 35**,** 1417-25.
EHRMANN, J., JR., MALINSKY, J. & GREGAR, I. 1990. Paneth cells and coeliac disease--quantitative, morphometric analysis. *Acta Univ Palacki Olomuc Fac Med,* 126**,** 187-201.
ESTES, J. D., HARRIS, L. D., KLATT, N. R., TABB, B., PITTALUGA, S., PAIARDINI, M., BARCLAY, G. R., SMEDLEY, J., PUNG, R., OLIVEIRA, K. M., HIRSCH, V. M., SILVESTRI, G., DOUEK, D. C., MILLER, C. J., HAASE, A. T., LIFSON, J. & BRENCHLEY, J. M. 2010. Damaged intestinal epithelial integrity linked to microbial translocation in pathogenic simian immunodeficiency virus infections. *PLoS Pathog,* 6**,** e1001052.
GALLO, A., TALERICO, R., NOVELLO, L., GIUSTINIANI, M. C., D'ARGENTO, E., BRIA, E. & MONTALTO, M. 2021. Collagenous colitis and atezolizumab therapy: an atypical case. *Clin J Gastroenterol,* 14**,** 165-169.
GANZ, T. 2000. Paneth cells--guardians of the gut cell hatchery. *Nat Immunol,* 1**,** 99-100.
GARABEDIAN, E. M., ROBERTS, L. J., MCNEVIN, M. S. & GORDON, J. I. 1997. Examining the role of Paneth cells in the small intestine by lineage ablation in transgenic mice. *J Biol Chem,* 272**,** 23729-40.
GASSLER, N. 2017. Paneth cells in intestinal physiology and pathophysiology. *World J Gastrointest Pathophysiol,* 8**,** 150-160.
GAUDINO, S. J., BEAUPRE, M., LIN, X., JOSHI, P., RATHI, S., MCLAUGHLIN, P. A., KEMPEN, C., MEHTA, N., ESKIOCAK, O., YUEH, B., BLUMBERG, R. S., VAN

DER VELDEN, A. W. M., SHROYER, K. R., BIALKOWSKA, A. B., BEYAZ, S. & KUMAR, P. 2021. IL-22 receptor signaling in Paneth cells is critical for their maturation, microbiota colonization, Th17-related immune responses, and anti-Salmonella immunity. *Mucosal Immunol,* 14**,** 389-401.

GUNAWARDENE, A. R., CORFE, B. M. & STATON, C. A. 2011. Classification and functions of enteroendocrine cells of the lower gastrointestinal tract. *Int J Exp Pathol,* 92**,** 219-31.

HIRAO, L. A., GRISHINA, I., BOURRY, O., HU, W. K., SOMRIT, M., SANKARAN-WALTERS, S., GAULKE, C. A., FENTON, A. N., LI, J. A., CRAWFORD, R. W., CHUANG, F., TARARA, R., MARCO, M. L., BAUMLER, A. J., CHENG, H. & DANDEKAR, S. 2014. Early mucosal sensing of SIV infection by paneth cells induces IL-1beta production and initiates gut epithelial disruption. *PLoS Pathog,* 10**,** e1004311.

HOLLY, M. K., DIAZ, K. & SMITH, J. G. 2017. Defensins in Viral Infection and Pathogenesis. *Annu Rev Virol,* 4**,** 369-391.

IMHOF, A., FROEHLICH, M., BRENNER, H., BOEING, H., PEPYS, M. B. & KOENIG, W. 2001. Effect of alcohol consumption on systemic markers of inflammation. *Lancet,* 357**,** 763-7.

IYER, N. & VAISHNAVA, S. 2016. Alcohol Lowers Your (Intestinal) Inhibitions. *Cell Host Microbe,* 19**,** 131-3.

JOHANSON, J. F. 1996. Diagnosis and management of AIDS-related diarrhea. *Can J Gastroenterol,* 10**,** 461-8.

KALLINGS, L. O. 2008. The first postmodern pandemic: 25 years of HIV/ AIDS. *J Intern Med,* 263**,** 218-43.

KARLSSON, J., PUTSEP, K., CHU, H., KAYS, R. J., BEVINS, C. L. & ANDERSSON, M. 2008. Regional variations in Paneth cell antimicrobial peptide expression along the mouse intestinal tract. *BMC Immunol,* 9**,** 37.

KELLY, P., FEAKINS, R., DOMIZIO, P., MURPHY, J., BEVINS, C., WILSON, J., MCPHAIL, G., POULSOM, R. & DHALIWAL, W. 2004. Paneth cell granule depletion in the human small intestine under infective and nutritional stress. *Clin Exp Immunol,* 135**,** 303-9.

KHALOIAN, S., RATH, E., HAMMOUDI, N., GLEISINGER, E., BLUTKE, A., GIESBERTZ, P., BERGER, E., METWALY, A., WALDSCHMITT, N., ALLEZ, M. & HALLER, D. 2020. Mitochondrial impairment drives intestinal stem cell transition into dysfunctional Paneth cells predicting Crohn's disease recurrence. *Gut,* 69**,** 1939-1951.

KOTLER, D. P. 2005. HIV infection and the gastrointestinal tract. *AIDS,* 19**,** 107-17.

KOTLER, D. P., GAETZ, H. P., LANGE, M., KLEIN, E. B. & HOLT, P. R. 1984. Enteropathy associated with the acquired immunodeficiency syndrome. *Ann Intern Med,* 101**,** 421-8.

KWON, O., YU, W. D., SON, Y. S., JUNG, K. B., LEE, H. & SON, M. Y. 2022. Generation of Highly Expandable Intestinal Spheroids Composed of Stem Cells. *Int J Stem Cells,* 15**,** 104-111.

LENCER, W. I. 1998. Paneth cells: on the front line or in the backfield? *Gastroenterology,* 114**,** 1343-5.

LEWIN, S. R. & ROUZIOUX, C. 2011. HIV cure and eradication: how will we get from the laboratory to effective clinical trials? *AIDS,* 25**,** 885-97.

LIN, X., GAUDINO, S. J., JANG, K. K., BAHADUR, T., SINGH, A., BANERJEE, A., BEAUPRE, M., CHU, T., WONG, H. T., KIM, C. K., KEMPEN, C., AXELRAD, J., HUANG, H., KHALID, S., SHAH, V., ESKIOCAK, O., PARKS, O. B., BERISHA, A.,

MCALEER, J. P., GOOD, M., HOSHINO, M., BLUMBERG, R., BIALKOWSKA, A. B., GAFFEN, S. L., KOLLS, J. K., YANG, V. W., BEYAZ, S., CADWELL, K. & KUMAR, P. 2022. IL-17RA-signaling in Lgr5(+) intestinal stem cells induces expression of transcription factor ATOH1 to promote secretory cell lineage commitment. *Immunity,* 55**,** 237-253 e8.

LLENADO, R. A., WEEKS, C. S., COCCO, M. J. & OUELLETTE, A. J. 2009. Electropositive charge in alpha-defensin bactericidal activity: functional effects of Lys-for-Arg substitutions vary with the peptide primary structure. *Infect Immun,* 77**,** 5035-43.

LLOPIS, M., CASSARD, A. M., WRZOSEK, L., BOSCHAT, L., BRUNEAU, A., FERRERE, G., PUCHOIS, V., MARTIN, J. C., LEPAGE, P., LE ROY, T., LEFEVRE, L., LANGELIER, B., CAILLEUX, F., GONZALEZ-CASTRO, A. M., RABOT, S., GAUDIN, F., AGOSTINI, H., PREVOT, S., BERREBI, D., CIOCAN, D., JOUSSE, C., NAVEAU, S., GERARD, P. & PERLEMUTER, G. 2016. Intestinal microbiota contributes to individual susceptibility to alcoholic liver disease. *Gut,* 65**,** 830-9.

LUESCHOW, S. R. & MCELROY, S. J. 2020. The Paneth Cell: The Curator and Defender of the Immature Small Intestine. *Front Immunol,* 11**,** 587.

MAH, A. T., VAN LANDEGHEM, L., GAVIN, H. E., MAGNESS, S. T. & LUND, P. K. 2014. Impact of diet-induced obesity on intestinal stem cells: hyperproliferation but impaired intrinsic function that requires insulin/IGF1. *Endocrinology,* 155**,** 3302-14.

MCCANCE-KATZ, E. F., GRUBER, V.A., BEATTY, G., LUM, P.J. AND RAINEY, P.M 2016. Interactions between alcohol and the antiretroviral medications ritonavir or efavirenz. *Journal of addiction medicine,* 7(4)**,** p.264.

MCCAULEY, H. A., MATTHIS, A. L., ENRIQUEZ, J. R., NICHOL, J. T., SANCHEZ, J. G., STONE, W. J., SUNDARAM, N., HELMRATH, M. A., MONTROSE, M. H., AIHARA, E. & WELLS, J. M. 2020. Enteroendocrine cells couple nutrient sensing to nutrient absorption by regulating ion transport. *Nat Commun,* 11**,** 4791.

MEI, X., GU, M. & LI, M. 2020. Plasticity of Paneth cells and their ability to regulate intestinal stem cells. *Stem Cell Res Ther,* 11**,** 349.

MONACO, C. L., GOOTENBERG, D. B., ZHAO, G., HANDLEY, S. A., GHEBREMICHAEL, M. S., LIM, E. S., LANKOWSKI, A., BALDRIDGE, M. T., WILEN, C. B., FLAGG, M., NORMAN, J. M., KELLER, B. C., LUEVANO, J. M., WANG, D., BOUM, Y., MARTIN, J. N., HUNT, P. W., BANGSBERG, D. R., SIEDNER, M. J., KWON, D. S. & VIRGIN, H. W. 2016. Altered Virome and Bacterial Microbiome in Human Immunodeficiency Virus-Associated Acquired Immunodeficiency Syndrome. *Cell Host Microbe,* 19**,** 311-22.

MUDGAL, M. M., BIRUDUKOTA, N. & DOKE, M. A. 2018. Applications of Click Chemistry in the Development of HIV Protease Inhibitors. *Int J Med Chem,* 2018**,** 2946730.

NEGIN, J. & CUMMING, R. G. 2010. HIV infection in older adults in sub-Saharan Africa: extrapolating prevalence from existing data. *Bull World Health Organ,* 88**,** 847-53.

O'FARRELLY, C. 2000. Is villous atrophy always and only the result of gluten sensitive disease of the intestine? *Eur J Gastroenterol Hepatol,* 12**,** 605-8.

PANDREA, I., HAPPEL, K. I., AMEDEE, A. M., BAGBY, G. J. & NELSON, S. 2010. Alcohol's role in HIV transmission and disease progression. *Alcohol Res Health,* 33**,** 203-18.

PARK, J. H., JUNG, I. K., LEE, Y., JIN, S., YUN, H. J., KIM, B. W. & KWON, H. J. 2021. Alcohol stimulates the proliferation of mouse small intestinal epithelial cells via Wnt signaling. *Biochem Biophys Res Commun,* 534**,** 639-645.

PERSSON, J. 1991. Alcohol and the small intestine. *Scand J Gastroenterol,* 26**,** 3-15.

PINTO, D. & CLEVERS, H. 2005. Wnt, stem cells and cancer in the intestine. *Biol Cell,* 97**,** 185-96.

PLUSKE, J. R., THOMPSON, M. J., ATWOOD, C. S., BIRD, P. H., WILLIAMS, I. H. & HARTMANN, P. E. 1996. Maintenance of villus height and crypt depth, and enhancement of disaccharide digestion and monosaccharide absorption, in piglets fed on cows' whole milk after weaning. *Br J Nutr,* 76**,** 409-22.

SALZMAN, N. H., HUNG, K., HARIBHAI, D., CHU, H., KARLSSON-SJOBERG, J., AMIR, E., TEGGATZ, P., BARMAN, M., HAYWARD, M., EASTWOOD, D., STOEL, M., ZHOU, Y., SODERGREN, E., WEINSTOCK, G. M., BEVINS, C. L., WILLIAMS, C. B. & BOS, N. A. 2010. Enteric defensins are essential regulators of intestinal microbial ecology. *Nat Immunol,* 11**,** 76-83.

SAMET, J. H., CHENG, D. M., LIBMAN, H., NUNES, D. P., ALPEREN, J. K. & SAITZ, R. 2007. Alcohol consumption and HIV disease progression. *J Acquir Immune Defic Syndr,* 46**,** 194-9.

SHANKMAN, L. S., FLEURY, S. T., EVANS, W. B., PENBERTHY, K. K., ARANDJELOVIC, S., BLUMBERG, R. S., AGAISSE, H. & RAVICHANDRAN, K. S. 2021. Efferocytosis by Paneth cells within the intestine. *Curr Biol,* 31**,** 2469-2476 e5.

SOMMERS, S. C. 1966. Mast cells and paneth cells in ulcerative colitis. *Gastroenterology,* 51**,** 841-50.

Simmonds, N., Furman, M., Karanika, E., Phillips, A. and Bates, A.W., 2014. Paneth cell metaplasia in newly diagnosed inflammatory bowel disease in children. BMC gastroenterology, 14(1), pp.1-6.

Tanaka, M., Saito, H., Kusumi, T., Fukuda, S., Shimoyama, T., Sasaki, Y., Suto, K., Munakata, A. and Kudo, H., 2001. Spatial distribution and histogenesis of colorectal Paneth cell metaplasia in idiopathic inflammatory bowel disease. Journal of gastroenterology and hepatology, 16(12), pp.1353-1359.

Symonds, D.A., 1974. Peneth cell metaplasia in diseases of the colon and rectum. Arch Pathol, 97, pp.343-347.

STRAUCH, U. & SCHOLMERICH, J. 1996. [Villous atrophy of the small intestine and iron deficiency]. *Dtsch Med Wochenschr,* 121**,** 1446.

TOBI, M., TALWAR, H. & MCVICKER, B. 2021. The Celiac Disease Microbiome Depends on the Paneth Cells of the Puzzle. *Gastroenterology,* 161**,** 359.

VOSHAVAR, C. 2019. Protease Inhibitors for the Treatment of HIV/AIDS: Recent Advances and Future Challenges. *Curr Top Med Chem,* 19**,** 1571-1598.

WANG, L., FOUTS, D. E., STARKEL, P., HARTMANN, P., CHEN, P., LLORENTE, C., DEPEW, J., MONCERA, K., HO, S. B., BRENNER, D. A., HOOPER, L. V. & SCHNABL, B. 2016. Intestinal REG3 Lectins Protect against Alcoholic Steatohepatitis by Reducing Mucosa-Associated Microbiota and Preventing Bacterial Translocation. *Cell Host Microbe,* 19**,** 227-39.

WINDON, A. L., ALMAZAN, E., OLIVA-HEMKER, M., HUTCHINGS, D., ASSARZADEGAN, N., SALIMIAN, K., MONTGOMERY, E. A. & VOLTAGGIO, L.

2020. Lymphocytic and collagenous colitis in children and adolescents: Comprehensive clinicopathologic analysis with long-term follow-up. *Hum Pathol,* 106**,** 13-22.
YOKOI, Y., NAKAMURA, K., YONEDA, T., KIKUCHI, M., SUGIMOTO, R., SHIMIZU, Y. & AYABE, T. 2019. Paneth cell granule dynamics on secretory responses to bacterial stimuli in enteroids. *Sci Rep,* 9**,** 2710.
YU, J., ZENG, Y., ZHAO, J., LIAO, D. & GREGERSEN, H. 2004. Quantitative analysis of collagen fiber angle in the submucosa of small intestine. *Comput Biol Med,* 34**,** 539-50.
ZAPATA, W., RODRIGUEZ, B., WEBER, J., ESTRADA, H., QUINONES-MATEU, M. E., ZIMERMMAN, P. A., LEDERMAN, M. M. & RUGELES, M. T. 2008. Increased levels of human beta-defensins mRNA in sexually HIV-1 exposed but uninfected individuals. *Curr HIV Res,* 6**,** 531-8.
ZARAGOZA, M. M., SANKARAN-WALTERS, S., CANFIELD, D. R., HUNG, J. K., MARTINEZ, E., OUELLETTE, A. J. & DANDEKAR, S. 2011. Persistence of gut mucosal innate immune defenses by enteric alpha-defensin expression in the simian immunodeficiency virus model of AIDS. *J Immunol,* 186**,** 1589-97.
ZEITZ, M., ULLRICH, R., SCHNEIDER, T., KEWENIG, S., HOHLOCH, K. & RIECKEN, E. O. 1998. HIV/SIV enteropathy. *Ann N Y Acad Sci,* 859**,** 139-48.
ZENG, Y. J., QIAO, A. K., YU, J. D., ZHAO, J. B., LIAO, D. H., XU, X. H. & HANS, G. 2003. Collagen fiber angle in the submucosa of small intestine and its application in Gastroenterology. *World J Gastroenterol,* 9**,** 804-7.
ZHOU, H., ZHOU, S. Y., GILLILLAND, M., 3RD, LI, J. Y., LEE, A., GAO, J., ZHANG, G., XU, X. & OWYANG, C. 2020. Bile acid toxicity in Paneth cells contributes to gut dysbiosis induced by high-fat feeding. *JCI Insight,* 5.
ZOUBI, S. A., MAYHEW, T. M. & SPARROW, R. A. 1994. Crypt and villous epithelial cells in adult rat small intestine: numerical and volumetric variation along longitudinal and vertical axes. *Epithelial Cell Biol,* 3**,** 112-8.

Appendix 1.

STUDY BUDGET

ITEM		RATE	COST
1	Slide mic	5	R15x5 =75
2	Cover slip 22x50ml	2	R79x2 = 158
3	Haematoxilin	1	R1103
4	Eosin	1	R529
5	Wiegert's working haematoxilin	1	R2540
6	Bouin's solution	1	R1926
7	Bierbrich scarlet	1	R2240
8	Phosphotonstic acid	1	R278
9	Ethanol	1	R686
10	Xyline	1	R236
11	ABC kit	1	R6703.89
12	Anti-alpha Defencins 5 antibody	1	R9780.72
13	Anti-lysozyme anti body	1	R10094.88
14	Anti-Musashi -1 anti-body	1	R10291.23
15	Goat Anti-Mouse IgG H&L	1	R2716.52
16	Goat Anti-Rabbit IgG H%L	1	R2716.52
17	Normal Goat serum	1	R4693.15
Total			R56692.91

Appendix 2.

Group A: (Negative control) (n=8): This group was fed normal chow and treated with a once off intraperitoneal injection of normal saline throughout the experimental days for 90 days.

Group B: Alcohol alone (n= 8): This group was fed normal rat chow and received 10% v/v ethanol in drinking water daily for 90 days.

Group C: cART alone (n= 8): This group was fed normal rat chow and treated cART at a dose of 23.22 mgAI/kgBW/day in gelatine cubes daily for 90 days

Group D: (n=8): This group received 10% alcohol and cART at a dose of 23.22 mgAI/kgBW/day

- Average adolescent from 12 years to 50 years =45kg body weight (BW)
- 1 Atripla tablet =1045mg Active Ingredient(AI) per day (600mg+200+245)

  1kg BW=1045mgAI per day ÷45=23.22mgAI/kgBW per day

DATA COLLECTING SHEET FOR MICROSCOPY					
i.	Paneth cells	Groups			
		Group A	Group B	Group C	Group D
	Present				
	Absent				
	Average number in 3 crypts				
ii.	Intest. stem cells	Groups			
		Group A	Group B	Group C	Group D
	Present				
	Absent				
	Average density in 3 crypts				
iii.	Crypt villous development	Groups			
		Group A	Group B	Group C	Group D
	Number of villi				
	Number of crypts				
	Average crypt width				
	Average crypt depth				
	Average crypt height				
	Villous height and width				

Appendix. 3.

Tissue preparation, processing, and sectioning

Obtaining a specimen: A fresh or a preserved tissue specimen will be received from a surgery department.

1. Fixation.
   The tissue will be fixed in 10 % phosphate-buffered formalin.
2. Grossing: Assessment of received tissue, further dissection to select appropriate areas for examination by placing on to a cassette, and the batch will be loaded on to an automated instrument called "Tissue Processor" for processing.
3. Processing: Involve dehydration and clearing of the tissue in a sequence of different solvent, finishing with paraffin/wax infiltration.

   Dehydration.

   1.50% ethanol in 10min.
   2. 70% ethanol in 10 min.
   3. 80% ethanol in 10min.
   4. 95% ethanol in 10 min.
   5. 100% ethanol in 10 min
   6. 100% ethanol in 10 min.

   Clearing

   Using Xylene to displace the ethanol in the tissue in the following sequence

   1. 2:1 ethanol: Xylene 20min

2. 1:1 ethanol: Xylene 20min
3. 1:2 ethanol: Xylene 45 min.
4. 100$ xylene 10-15min
5. 100% xylene 10-15min
6. 100% xylene 10-15min.
7. Exchange of Xylene with paraffin

This step will be carried out in a vacuum oven set at 54-58^{o}C.Paraplast X-tra or Paraplast plus.

2;1 Xylene: Paraffin 30min

1:1 Xylene: Paraffin 30min

1:2 xylenes: Paraffin 30min

100% Paraffin 1-2hr

100% Paraffin 1-2 hr. or overnight

4. Wax infiltration/Paraffin embedding
    1. Warm the wax as well as the metal molds at temperature, not more than 60^{o}C.
    2. Fill the metal mold with melted wax.
    3. Embed a tissue in fresh new paraffin and orient tissue as desired for easy sectioning
    4. Cool the paraffin-embedded tissue block on ice before sectioning.

       Sectioning.
    5. Place the blade in the holder and ensure it is secure.
    6. Approach the blade to the paraffin-block, and carefully cut the section at a thickness of 5µm.
    7. Using tweezers pick up the ribbons of sections and float the in the surface of the water so they flatten out.
    8. To use microscope slides to pick up the sections out of the water and store in a slide rack.
    9. Place the slide rack into an oven and allow to dry overnight a room temperature.

Appendix 4.

Hematoxylin and Eosin staining.

Reagents.

Eosin Y solution

Ethanol (100%, 95%, 70%).

Hematoxylin solution

Per mount mounting medium.

Xylene

Equipment.

Coverslips

Glass Slides

Glass or Metal staining dish

Microscope.

Before beginning the procedure, the tissue shall be embedded in paraffin, sectioned to 5µm in a water bath, and picked up on the glass slide, and after that placed on slide racks.

1. Glass slides holding the paraffin section will be placed in staining racks. The paraffin from the sample will be clear in three changes of xylene for about 2 min per change.
2. Hydration of samples as follows
3. I- Transfer the slides through changes of ethanol 100% for 2 min per change
   I- Transfer to ethanol 95% for 2 min
   II- Transfer to ethanol 70% foe 2 min
   III- To rinse in running tap water for at least 5 min.
4. Stain by using Mayer's Hematoxylin solution for 10 min.
5. Put the slide under running tap water for 5min
6. Blue in Scott's tap water for 2min
7. Wash in running tap water for 2 min
8. Stain the sample I Eosin for 2 min
9. Wash in tap water for 2 min
10. Dehydrate the sample as follows:
    I. Dip in 70% ethanol for 15min
    II. Dip in 90% ethanol for 15min
    III. Dip in 100% ethanol for 15 min.
    IV. Dip in 100% ethanol for 30 min
    V. Dip in 100% ethanol for 45min
    VI. Clear the sample in three changes of xylene for 20min, 20min and 45 min per change.
    VII. Place a drop of paramount over the tissue on each slide and add cove slip.
    VIII. Mount

Appendix 5.

Masson's Trichrome Staining.

1. Stain the deparaffinize section in Hansen's iron hematoxylin for 1-5min.
2. Wash in tap water until picric acid is removed expected after 5 min.
3. Stain in Masson's Fuchsin-Ponceau mixture, 10 times diluted with water to 0.2 percent with acetic acid for 5 min.
4. Rinse in distilled water or tap water if not too alkaline.
5. Treat with Phosphotongstic acid orange G for 15 secs to 30 min.
6. Rinse in distilled water/tap water.
7. Stain in Masson's light green solution diluted 10 times with water, approximately for 5 min.
8. Rinse in distilled water for 5 min.
9. Dehydrate in the usual manner with ethanol in ascending percentage.
10. Clear in xylene, and mount in balsam and cover slip.

Appendix 6

Alcian Blue and PAS Staining

1. Bring sections to distilled water.
2. Stain with Alcian blue 15 mins
3. Wash well in running tap water 2 mins
4. Rinse in distilled water
5. Treat with periodic acid 5 mins
6. Wash well in distilled water
7. Stain with Schiff's reagent 10 mins
8. Wash well in running tap water 5 mins
9. Stain nuclei with haematoxylin 1 min
10. Wash in running tap water 2 mins
11. Differentiate with acid alcohol
12. Wash and blue nuclei in Scott's tap water
13. Wash in water
14. Dehydrate, clear and mount.

Appendix 7.

Immunohistochemistry staining for anti-defencins5, and Musashi-1.

Materials and reagent.

Peroxidase block

- 0.2M phosphate buffer
- 8ml methanol
- 80µl Triton X100.
- 2 ml hydrogen peroxide

Blocking buffer

- 0.1M phosphate buffer
- 0.3 % Triton.
- 1 % serum from secondary antibodies host species.

1. To deparaffinize the section in xylene and rehydrate in ethanol at graded series.
2. To pretreat the section using heat-mediated antigen retrieval by incubation in a sodium citrate buffer solution (100mM sodium citrate, 0.05% Tween 20, PH 6.0) overnight at a temperature of 60^0C.
3. To Rinse slides in PBS three times for 15min.
4. To deactivate endogenous peroxidase by using 1% H2O2 for 20min with gentle agitation.
5. To Rinse slides in PBS three times for 15min
6. To incubate the section with 5% normal goat serum 30 minutes.
7. Tap serum of slides. Do not wash
8. To add Primary antibody, Anti-Musashi1 antibody in a dilution 1:500 or anti-Alpha defensin 5 in a dilution1:200, and incubate overnight at 4^{o}C.
9. To wash slides in PBS three times for 15min.
10. Incubate with secondary antibody (biotinylated goat anti-rabbit, anti-mouse; Vector labs;1:1000 30 mins
11. To wash slides in PBS three times for 15min.
12. To add Avidin-biotin complex reagent (ABC KIT) in TBS for 30 min at a room temperature
13. To wash slides in PBS three times for 15min.

14. To Pre-incubate the section for DAB reaction (diaminobenzidine tetrachloride substrate kit) in solution 0.5mg/ml in TB (PH7.6) using 2ml per vial and monitor the reaction under microscope and reaction will be stopped if the background staining appears brown

15 To wash slides in PBS three times for 15min.

16. To dehydrate the section in three graded series of alcohol, clear in 2 changes of xylene.

17. To counterstain the section with hematoxylin for 30 sec.

18. To mounted section with mounting medium entellen and cover with a seal coverslip prevent drying and movement under microscope.

19. Observe the reaction using light microscope

20. To air-dry the slides in a fume hood overnight

Appendix 8

	Jejunum	**Ileum**
Mean number of villi		
Group A	27.38±1.97	13±1.29
Group B	42.00±1.95	38.25±1.97
Group C	41.71±2.31	37.71±4.31
Group D	20.33±3.78	12.67±1.18
Mean number of crypts		
Group A	46.38±11.43	16±1.2
Group B	103.75±1.77	90.88±8.55
Group C	57.86±5.37	56±3.76
Group D	63.33±12.63	61.67±10.34
Mean villous Height		
Group A	478.88±120.25	465.88±51.65
Group B	282.75±87.26	230.38±26.10
Group C	260.14±40.25	214.14±54.34
Group D	652.00±110.75	642.33±36.30
Mean villous width		
Group A	109.50±14.57	132.5±7.15
Group B	61.13±10.71	57.63±17.70
Group C	61.00±9.37	79.29±10.45
Group D	146.00±18.08	183.67±38.23
Mean crypts depth		
Group A	130.13±24.59	95.13±16.23
Group B	107.88±21.43	80.25±11.90
Group C	56.57±8.88	57.86±10.25
Group D	247.00±17.65	278.67±8.22
Mean crypts width		
Group A	64±6.54	51.13±2.14

Group B	33.88±3.59	24.13±4.43
Group C	32.57±1.86	19.29±6.85
Group D	96±10.70	61.33±5.65
Mean wall thickness		
Group A	134.50±16.47	184.88±11.31
Group B	77.13±10.10	99.00±13.95
Group C	80.00±14.65	82.29±14.23
Group D	139.33±9.67	146.33±8.81

Histomorphometry Changes in the Small Intestinal Epithelium and Paneth Cells TURNITIN.docx

ORIGINALITY REPORT

13%	10%	9%	7%
SIMILARITY INDEX	INTERNET SOURCES	PUBLICATIONS	STUDENT PAPERS

PRIMARY SOURCES

1	www.ncbi.nlm.nih.gov Internet Source	3%
2	Elinore F. McCance-Katz, Valerie A. Gruber, George Beatty, Paula J. Lum, Petrie M. Rainey. "Interactions Between Alcohol and the Antiretroviral Medications Ritonavir or Efavirenz", Journal of Addiction Medicine, 2013 Publication	2%
3	pubs.niaaa.nih.gov Internet Source	2%
4	www.aidsmap.com Internet Source	1%
5	www.hindawi.com Internet Source	1%
6	Martin F. Graham, Robert F. Diegelmann, Charles O. Elson, William J. Lindblad, Nancy Gotschalk, Steffen Gay, Renate Gay. "Collagen	1%

	content and types in the intestinal strictures of Crohn's disease", Gastroenterology, 1988 Publication	
7	www.nature.com Internet Source	1 %
8	Ouellette, AndrÃ© J.. "Paneth Cells", Physiology of the Gastrointestinal Tract Two Volume Set, 2012. Publication	1 %
9	ujcontent.uj.ac.za Internet Source	1 %
10	www.jscholaronline.org Internet Source	1 %
11	Robert D. Cardiff, Claramae H. Miller, Robert J. Munn. "Manual Hematoxylin and Eosin Staining of Mouse Tissue Sections", Cold Spring Harbor Protocols, 2014 Publication	1 %
12	hdl.handle.net Internet Source	1 %
13	Submitted to Higher Education Commission Pakistan Student Paper	1 %

Please note that only typewritten applications will be accepted.

UNIVERSITY OF THE WITWATERSRAND

ANIMAL ETHICS SCREENING COMMITTEE

MODIFICATIONS AND EXTENSIONS TO EXPERIMENTS

a. Name: DR. I EGUAVOEN

Email address: dr_idemudia@yahoo.com

b. Department/School: Anatomical Science

c. Experiment to be modified / extended

		AESC NO	
Original AESC number			
Protocol Approval No		2018/11/58/C	
Other M&Es :			

d. **Project Title**: Diabetic skeletopathy of the Sprague- Dawley rat mandible in chronic alcohol intake and antiretroviral therapy: An immunohistochemical and micro-focus X-ray computed tomography study

		No.	Species
e.	Number and species of animals originally approved:	120	Male Sprague Dawley rats
f.	Number of additional animals previously allocated on M&Es:	Nil	
g.	Total number of animals allocated to the experiment to date:	82	
h.	Number of animals used to date:	82	

i. Specific modification / extension requested:

Inclusion of **ZEKHETHELO LETICIA MASEKO, student registration number: 183 76 47** as co-worker for **Master's degree project**. Student will use the SMALL INTESTINE of rats from the 4 groups: Control, Atripla alone, Alcohol alone, Alcohol and Atripla treated groups in the study for the purpose of her Master's degree project under the supervision of Dr. P. Mazengenya, and Co-supervisors, Prof. T Luvhengo and Prof. Felix E. Mbajiorgu. Prof Mbajiorgu is included in the original ethics certificate, but Dr. P. Mazengenya, and Prof. T Luvhengo are to be included in the M&E as co-workers to be able to supervise this study because of their specialty in the field of study.

This student will use already harvested SMALL INTESTINE for the study on the analysis of the effects of Atripla and Alcohol on the Paneth Cells in the Small Intestine, which DOES NOT involve any animal treatment or the use of CAS.

Date: 18/08/ 2020 Signature:

RECOMMENDATIONS

Approval for the addition of co-workers Z. Maseko (Student number 1837647), Dr. P. Mazengenya and Prof. T. Luvhengo to the study. Approval of Z. Maseko to use previously stored small intestine samples for their MSc study.

Date: 1 October 2020 Signature:

Deputy-Chair